

1 **RESEARCH ARTICLE**

2
3 **Molecular dissection of an intronic enhancer governing cold-induced**
4 **expression of the vacuolar invertase gene in potato**

5
6 **Xiaobiao Zhu^{1,2,*§}, Airu Chen^{1,*}, Nathaniel M. Butler^{2,3,*}, Zixian Zeng^{2,4,5}, Haoyang Xin⁶,**
7 **Lixia Wang¹, Zhaoyan Lv¹, Dani Eshel⁷, David S. Douches^{8,9}, and Jiming Jiang^{2,6,9,10,§}**
8
9

10 ¹ Anhui Province Key Laboratory of Horticultural Crop Quality Biology, School of Horticulture, Anhui
11 Agricultural University, Hefei 230036, Anhui Province, China

12 ² Department of Horticulture, University of Wisconsin-Madison, Madison, Wisconsin 53706, USA

13 ³ United States Department of Agriculture-Agricultural Research Service, Vegetable Crops Research
14 Unit, Madison, Wisconsin 53706, USA

15 ⁴ Department of Biological Science, College of Life Sciences, Sichuan Normal University, Chengdu
16 610101, Sichuan Province, China

17 ⁵ Plant Functional Genomics and Bioinformatics Research Center, Sichuan Normal University, Chengdu
18 610101, Sichuan Province, China

19 ⁶ Department of Plant Biology, Michigan State University, East Lansing, Michigan 48824, USA

20 ⁷ Department of Postharvest Science, The Volcani Institute, ARO, Rishon LeZion, Israel

21 ⁸ Department of Plant, Soil, and Microbial Sciences, Michigan State University, East Lansing, Michigan
22 48824, USA

23 ⁹ Michigan State University AgBioResearch, East Lansing, Michigan 48824, USA

24 ¹⁰ Department of Horticulture, Michigan State University, East Lansing, Michigan 48824, USA

25 * These authors contributed equally to this work.

26
27 **Short title:** Enhancer-mediated response to cold temperature
28
29
30
31

32 [§] Corresponding authors: Xiaobiao Zhu (xiaobiao11302005@163.com) and Jiming Jiang
33 (jiangjm@msu.edu)

34
35
36 The author responsible for distribution of materials integral to the findings presented in this article in
37 accordance with the policy described in the Instructions for Authors
38 (<https://academic.oup.com/plcell/pages/General-Instructions>) is Jiming Jiang
39 (jiangjm@msu.edu).
40
41

42 **Abstract**

43 Potato (*Solanum tuberosum*) is the third most important food crop in the world. Potato tubers
44 must be stored at cold temperatures to minimize sprouting and losses due to disease. However,
45 cold temperatures strongly induce the expression of the potato vacuolar invertase gene (*VInv*)
46 and cause reducing sugar accumulation. This process, referred to as “cold-induced sweetening”,
47 is a major postharvest problem for the potato industry. We discovered that the cold-induced
48 expression of *VInv* is controlled by a 200-bp enhancer, *VInvIn2En*, located in its second intron.
49 We identified several DNA motifs in *VInvIn2En* that bind transcription factors involved in the
50 plant cold stress response. Mutation of these DNA motifs abolished *VInvIn2En* function as a
51 transcriptional enhancer. We developed *VInvIn2En* deletion lines in both diploid and tetraploid
52 potato using clustered regularly interspaced short palindromic repeat (CRISPR)/CRISPR-
53 associated nuclease 9 (Cas9)-mediated gene editing. *VInv* transcription in cold-stored tubers was
54 significantly reduced in the deletion lines. Interestingly, the *VInvIn2En* sequence is highly
55 conserved among distantly related *Solanum* species, including tomato (*Solanum lycopersicum*)
56 and other non-tuber-bearing species. We conclude that the *VInv* gene as well as the *VInvIn2En*
57 enhancer have adopted distinct roles in the cold stress response in tubers of tuber-bearing
58 *Solanum* species.

59
60 Keywords: enhancer, intron, vacuolar invertase, cold-induced sweetening

61

62 Introduction

63 Potato (*Solanum tuberosum*) is the third most important food crop in the world in terms of
64 human consumption (Devaux et al., 2020). In addition, French fries and potato chips are among
65 the most consumed snacks, especially in developed countries. Unlike the grain crops, storage is
66 one of the most important issues related to the potato industry because tubers must be stored at
67 cold temperatures to prevent sprouting and diseases. Unfortunately, cold storage triggers the
68 breakdown of starch and accumulation of reducing sugars, which is referred to as “cold-induced
69 sweetening” (CIS) (Dale and Bradshaw, 2003), a costly and nagging problem for the potato
70 processing industry (Sowokinos, 2001). The reducing sugars in tubers will react with free amino
71 acids via a nonenzymatic, Maillard-type reaction during high-temperature processing. This
72 reaction results in products with dark color and bitter taste and produces acrylamide, a potential
73 carcinogen (Mottram et al., 2002; Stadler et al., 2002). Reducing sugars are the primary
74 determinants for the acrylamide content in fried potato products (Amrein et al., 2003; Becalski et
75 al., 2004; Zhu et al., 2016). Thus, developing methods to minimize reducing sugars in cold-
76 stored tubers has been an important research focus to reduce acrylamide in fried potato products.

77 CIS was reported to be associated with numerous genetic loci based on genetic mapping
78 (Menendez et al., 2002; Li et al., 2008; Braun et al., 2017), genome-wide association studies
79 (GWAS) (Byrne et al., 2020), and comparative proteomics studies between CIS-resistant and
80 CIS-susceptible potato cultivars (Fischer et al., 2013). This can be explained by the fact that CIS
81 is likely linked to numerous enzymes that function in central carbohydrate metabolism in potato
82 tubers (Sowokinos, 2001). The vacuolar invertase gene (*VInv*) received a major attention on its
83 potential role in CIS. Partial control of CIS was accomplished by manipulating the activity of the
84 VINV protein (Greiner et al., 1999; Agarwal et al., 2003) or the transcription of the *VInv* gene
85 (Zrenner et al., 1996; Zhang et al., 2008). Silencing of *VInv* using RNAi resulted in nearly full
86 control of CIS in at least some potato cultivars (Bhaskar et al., 2010; Ye et al., 2010).

87 Interestingly, *VInv* gene transcription in tubers is maintained at a minimal level under room
88 temperature. *VInv* is dramatically upregulated during cold storage in CIS-susceptible potato
89 cultivars (Zrenner et al., 1996; Bagnaresi et al., 2008; Bhaskar et al., 2010), causing rapid
90 accumulation of reducing sugars. Silencing of the *VInv* gene has been proven to be an effective
91 approach to control CIS in many potato cultivars (Bhaskar et al., 2010; Ye et al., 2010; Liu et al.,
92 2011; Wu et al., 2011; Clasen et al., 2016; Ly et al., 2023). Concordantly, overexpression of

93 *StInvInh2*, which encodes a vacuolar invertase inhibitor, can also reduce potato CIS (Liu et al.,
94 2013; Mckenzie et al., 2013).

95 Interestingly, the upregulation of *VInv* in cold-stored tubers is not controlled by its
96 promoter (Ou et al., 2013). The *VInv* promoter is required to respond to sugars, indole-3-acetic
97 acid (IAA), and gibberellic acid (GA₃), but not to cold temperatures (Ou et al., 2013). Here we
98 report discovery of a 200-bp transcriptional enhancer, *VInvIn2En*, located in the second intron of
99 *VInv*. This enhancer is responsible for the cold-induced expression of the *VInv* gene. We
100 identified several DNA motifs that bind transcription factors (TFs) involved in plant response to
101 cold stress. Mutation of these motifs abolished the function of *VInvIn2En*. We developed
102 *VInvIn2En* deletion lines in both diploid and tetraploid potato lines using CRISPR/Cas9-
103 mediated genome editing. *VInv* transcription was significantly reduced in the deletion lines
104 during cold storage. Interestingly, the *VInvIn2En* sequence was found to be highly conserved
105 among distantly related plant species, revealing an evolutionary trajectory of the *VInv* gene in
106 response to cold stress in the tuber-bearing *Solanum* species.

107

108 **Results**

109 **Discovery of a cold-responsive intronic enhancer within *VInv* gene**

110 Genomic regions containing active *cis*-regulatory elements (CREs), such as promoters
111 and transcriptional enhancers, can be identified as DNase I hypersensitive sites (DHSs) (Zhang et
112 al., 2012; Jiang, 2015; Zhao et al., 2018). We previously developed genome-wide DHS maps in
113 DM1-3 potato using chromatin isolated from tuber tissue (Zeng et al., 2019). DM1-3 is a
114 homozygous diploid clone and was developed from chromosome doubling of a monoploid
115 derived from an *S. tuberosum* Phureja Group clone (Mribu and Veilleux, 1990; Paz and Veilleux,
116 1999) and has been fully sequenced ($2n = 2x = 24$) (The Potato Genome Sequencing Consortium,
117 2011; Pham et al., 2020). We detected a 475-bp DHS within the second intron of *VInv* (**Figure**
118 **1A**), suggesting that this intron may play a role in regulation of the expression of *VInv*. We have
119 recently demonstrated the enhancer function of several intronic DHSs in *Arabidopsis*
120 (*Arabidopsis thaliana*) (Meng et al., 2021).

121 To confirm its *cis*-regulatory function, we cloned the entire *VInv* second intron (1,327 bp)
122 from RH potato, which is a heterozygous diploid clone (van Os et al., 2006) and has recently
123 been fully sequenced (Zhou et al., 2020). RH is susceptible to CIS (**Supplemental Figure S1**).

124 The intron was cloned into the pKGWFS 7.0 vector containing a minimal 35S promoter (-50 to -
125 2 bp) (m35S) and the β -glucuronidase (GUS) reporter gene (Zhu et al., 2015). Katahdin, a CIS-
126 susceptible tetraploid cultivar (Bhaskar et al., 2010), was used for transformation. We developed
127 20 transgenic Katahdin lines from the intron construct (*VInvIn2*) and 20 lines from a reverse
128 construct (*VInvIn2R*) in which the sequence orientation of the cloned intron is reversed. We
129 detected minimal GUS signals in transgenic tubers stored at room temperature (22°C). In
130 contrast, substantially enhanced GUS signals were detected in the transgenic tubers after 4 weeks
131 of cold storage (4°C) (**Figure 1B**). These results indicate that intron 2 of *VInv* contains an
132 enhancer that is responsible for its cold-induced expression.

133

134 **Dissection of intronic enhancer via reporter gene assays in *A. thaliana***

135 Since the entire intron 2 from RH potato was used for GUS reporter assays, the precise
136 size and position of the predicted enhancer within intron 2 could not be determined. We
137 attempted to fine-map the enhancer using reporter gene assay in *A. thaliana*. We first examined
138 the GUS signal profiles of transgenic *A. thaliana* plants using the *VInvIn2* and *VInvIn2R*
139 constructs. Consistent and strong GUS signals were detected in stems and petioles in transgenic
140 plants derived from both constructs. In addition, relatively weak and sporadic GUS signals were
141 also detected in roots (**Figure 2B**). The *VInv* gene is expressed at relatively high levels in several
142 non-tuber tissues of potato, including both petiole and stem (The Potato Genome Sequencing
143 Consortium, 2011; Zhou et al., 2020). Thus, the GUS signal patterns observed in the transgenic *A.*
144 *thaliana* plants correspond well with the *VInv* expression patterns in potato tissues.

145 We next divided the 1327-bp intron 2 into ten DNA fragments (#1 to #10) using five
146 breaks (b1 to b5, **Figure 2A**). Each fragment was ligated to the m35S promoter and cloned into
147 the pKGWFS 7.0 vector. Transgenic plants derived from DNA fragments #1, #2, #9, and #10
148 showed strong GUS signals in stems and petioles, which were similar to the transgenic plants
149 developed from the *VInvIn2* and *VInvIn2R* constructs. Similar but weaker signals were detected
150 from transgenic plants derived from fragment #8 (**Figure 2C**). These results indicated that the
151 enhancer driving *GUS* expression in stems and petioles is located between b2 and b4, which was
152 named fragment #11 (**Figure 2D**).

153 We next further divided the 600-bp fragment #11 into 13 sub-fragments (#12 to #24,
154 **Figure 2D**) for GUS reporter assays. Transgenic plants derived from construct #21 (200 bp)

155 showed strong GUS signals in stems and petioles. In contrast, transgenic plants derived from
156 constructs #17 and #19 did not show GUS signals (**Figure 2E**). Thus, the core enhancer in intron
157 2 was mapped within the 200-bp #21 sequence and was named as *VInvIn2En* thereafter.
158 *VInvIn2En* spans 678-877 bp in the intron and is located within the 475-bp DHS, which spans
159 597-1,071 bp in the intron (**Figure 1A**).

160 To confirm the function of *VInvIn2En* in potato, we developed transgenic lines using a
161 *VInvIn2En*-m35S-GUS construct in Katahdin potato. We detected minimal GUS signals in tubers
162 stored at room temperature (22°C) but strong GUS signals in cold-stored tubers (4°C) from three
163 independent transgenic lines (**Figure 2F**). Thus, the *VInvIn2En* sequence retains the same
164 function as the entire intron 2 in potato (**Figure 1B**).

165

166 **Identification of DNA motifs related to *VInvIn2En* function**

167 We speculated that *VInvIn2En* contains DNA motifs bound by TFs involved in plant
168 response to cold stress. We identified putative DNA motifs related to a total of 15 TFs in the
169 intron 2 sequence of RH (Zhou et al., 2020). These motifs were consistently detected by two
170 independent programs using both CIS-BP (Weirauch et al., 2014) and PlantPAN 3.0 (Chow et al.,
171 2019). Interestingly, 10 of these 15 TFs were previously reported to be associated with responses
172 to cold stress in one or multiple plant species (**Figure 3A**), including AT-hook (Dahro et al.,
173 2022), C2H2 ZF (He et al., 2019), MADS-box (Chen et al., 2019), NAC/NAM (Li et al., 2016),
174 bHLH (Xie et al., 2012), CBF/NF-Y (Zhou et al., 2022; Zhang et al., 2023), bZIP (Liu et al.,
175 2018; Li et al., 2022b), B3 (Verma and Bhatia, 2019), TCP (Li et al., 2022a), and GATA (Zhang
176 et al., 2021).

177 Several TF motifs were enriched in the 200-bp *VInvIn2En*, including bHLH and
178 CBF/NF-Y. In addition, motifs related to TCP and GATA were found only in the 200-bp
179 enhancer region (**Figure 3A**). We designed mutated versions of *VInvIn2En* to test the function of
180 the DNA motifs related to B3, bHLH, CBF/NF-Y, TCP and GATA. In each construct, the target
181 motif(s) were mutated by replacing 1-3 nucleotide(s) within the sequence (**Figure 3B**,
182 **Supplemental Table S1**). Transgenic *A. thaliana* plants using *VInvIn2En* with a mutated B3
183 motif showed similar GUS signal patterns as those from wild type *VInvIn2En*. Reduced GUS
184 signals were detected from transgenic plants using *VInvIn2En* with two mutated bHLH motifs. In
185 contrast, we did not detect any GUS signals from transgenic plants derived from the three

186 constructs with mutated motifs related to CBF/NF-Y, TCP, and GATA. Most strikingly, a single
187 nucleotide mutation within the GATA motif resulted in a complete loss of function of the
188 *VInvIn2En* enhancer (**Figure 3B**). These results indicated that CBF/NF-Y, TCP and GATA all
189 play important roles for *VInvIn2En* driving *GUS* expression in stems and petioles.

190 To seek additional functional evidence of the three DNA motifs identified in *VInvIn2En*,
191 we conducted a yeast one-hybrid (Y1H) assay using triple copies of the *VInvIn2En* sequence as a
192 bait (see Materials and Methods). A total of 387 yeast colonies were obtained by screening a
193 cDNA library developed from cold-treated tuber tissues from RH potato. All 387 clones were
194 fully sequenced. The sequences were used for BLAST search in the DM1-3 potato cDNA (v6.1)
195 database using Spud DB blastn program (<http://spuddb.uga.edu/blast.shtml>). All of the best
196 matched cDNA sequences with an E-value $<1e-5$ and a minimum sequence identity of 82% were
197 kept for further analyses. A total of 33 unique cDNA sequences were obtained after filtering out
198 repeated cDNA sequences. The candidate proteins related to these 33 cDNAs were used for
199 further validation using point-to-point Y1H assay (see Materials and Methods). Five proteins,
200 including StNF-YC1 and StNF-YC9 (**Figure 4**), were validated as positive interacting proteins
201 binding to *VInvIn2En*. The StNF-YC1 and StNF-YC9 proteins share 86% and 73% sequence
202 similarity with AtNF-YC1 and AtNF-YC9 of *A. thaliana*, respectively. These results validated
203 the predicted role of CBF/NF-Y family TFs in regulation of CIS mediated by the *VInvIn2En*
204 enhancer.

205

206 **Genome editing of *VInvIn2En* in diploid potato**

207 The *in vivo* function of a predicted enhancer can be validated by mutation or deletion
208 using genome editing (Meng et al., 2021; Zhao et al., 2022; Fang et al., 2023). We attempted to
209 develop *VInvIn2En* deletion lines in potato to validate its *in vivo* function. We first conducted
210 CRISPR/Cas experiments using a self-compatible diploid clone DMF5-73-1. This clone was
211 self-pollinated for five generations from a self-compatible diploid hybrid DM1-3 \times M6
212 (Endelman and Jansky, 2016). DMF5-73-1 is amenable to *Agrobacterium*-mediated
213 transformation (Butler et al., 2020). Five sgRNAs flanking *VInvIn2En* (1a, 2a, 3a, 1b and 2b) and
214 a single sgRNA (3b) targeting *VInvIn2En* (**Figure 5A, Supplemental Table S2**) were designed
215 and assembled into a single construct (**Supplemental Figure S2**). Primary transformants were
216 generated using a hairy root-based procedure to create stable CRISPR/Cas mutants in the first

217 generation (T0) (Butler et al., 2020). T0 events carrying targeted deletions were self-pollinated
218 and the progeny were screened for homozygous mutations (T1). We identified three homozygous
219 T1 deletion lines (**Figure 5B**). Two lines, 13-1-3 and 13-2-1, were derived from the same hairy
220 root culture. Sequencing analysis showed that deletion line 2-2-8 lost 369 bp, including the entire
221 200-bp *VInvIn2En*. Lines 13-1-3 and 13-2-1 lost 394 bp, including the first 122 bp of *VInvIn2En*
222 (**Supplemental Figure S3**), which spans the GATA and the three CBF/NF-Y motifs.

223 DMF5-73-1 is not susceptible to CIS and expresses a weak CIS phenotype. Tubers
224 harvested from the three deletion lines were stored at 12.8°C for 6 weeks followed by at 6.7°C
225 for nine additional weeks, a storage procedure used to maximize the CIS phenotype. Tuber
226 tissues were then sampled for RNA extraction and RT-qPCR analysis. We found that the
227 expression of *VInv* gene was reduced by 54% for 2-2-8, 45% for 13-1-3, and 41% for 13-2-1,
228 respectively, compared to the wild-type DMF5-73-1 (**Figure 5C**). However, it was challenging
229 to perform chipping analysis from the deletion lines because all three lines have small tubers and
230 are associated with the “jelly end” defect derived from the parental clone DM1-3 (Endelman and
231 Jansky, 2016) (**Figure 5D**). Nevertheless, potato chips processed from cold-stored tubers of line
232 13-1-3 showed a lighter color compared to those processed from wild-type DMF5-73-1 (**Figure**
233 **5D**).

235 **Genome editing of *VInvIn2En* in tetraploid potato**

236 DMF5-73-1 is ideal for CRISPR/Cas experiments due to its self-compatibility that allows
237 for identification of homozygous deletions. However, DMF5-73-1 is not an ideal line to
238 accurately evaluate the impact of *VInvIn2En* on CIS since it is resistant to CIS and has poor tuber
239 traits. In addition, DMF5-73-1 retains a significant level of heterozygosity. Hence, the
240 homozygous deletion lines developed from this clone are phenotypically different from the
241 parental DMF5-73-1 (**Figure 5D**). We next attempted to conduct CRISPR/Cas experiments in
242 Katahdin, a tetraploid potato cultivar that is highly susceptible to CIS (Bhaskar et al., 2010). We
243 first amplified and sequenced the intron 2 of *VInv* from Katahdin. We identified three haplotypes:
244 A (2 copies), B, and C. These haplotypes are differentiated by SNPs and small indels, including
245 those within the *VInvIn2En* region (**Supplemental Figure S4**). We designed four sgRNAs,
246 including R1 outside of *VInvIn2En*, and R2, R3, and R4 inside the *VInvIn2En* boundary (**Figure**

247 **5A, Supplemental Figure S4, Supplemental Table S2).** The four sgRNAs were assembled into
248 a single construct for CRISPR/Cas experiments (**Supplemental Figure S5**).

249 We identified three different T0 CRISPR/Cas9 lines, KV78, KV87, and KV108. PCR
250 amplifications using primers *VInv*-Edit-F/R that span the four sgRNAs (**Supplemental Figure**
251 **S4, Supplemental Table S3**) produced additional smaller bands as well as the wild-type band
252 (**Figure 5E**), suggesting that all three T0 lines contain both intact and deleted intron 2, possibly
253 derived from different lineages of cells. We then isolated and mixed all DNA fragments visible
254 on the agarose gel, including the wild-type band, from all three lines. The mixed DNA fragments
255 were cloned and a minimum of 60 randomly selected clones from each line were fully sequenced.
256 Sequence analysis confirmed that each of the three T0 lines contained different types of deletions
257 within *VInvIn2En*, ranging from 3 to 124 bp deletions within *VInvIn2En* associated with
258 haplotype A, and 1 to 15 bp deletions within *VInvIn2En* associated with haplotype B
259 (**Supplemental Figure S6**). However, no deletions were detected in *VInvIn2En* associated with
260 haplotype C, probably due to the SNPs located in the PAM sequences downstream of sgRNAs
261 R2 and R3. Based on the number of individual sequences related to *VInvIn2En*, 67.7% of the
262 haplotype A sequences from KV78 contained a deletion ranging from 4 to 97 bp; 64.7% of the
263 haplotype A sequences from KV87 contained a deletion of 3 to 64 bp; 59.3% of the haplotype A
264 sequences from KV108 contained a 4 to 124 bp deletion (**Supplemental Figure S6**).

265 We amplified the cDNAs of *VInv* from the three CRISPR/Cas lines using primers
266 Splicing-F/R spanning exons 1 to 3 (**Supplemental Table S3**). Sequencing of the PCR products
267 showed that the transcripts from the three CRISPR/Cas lines were identical to those from wild-
268 type Katahdin (**Figure 5F**). Thus, the deletions occurred in *VInvIn2En* did not affect the splicing
269 of the *VInv* gene. We next analyzed the expression of the *VInv* gene in the three CRISPR/Cas
270 lines using RNAs isolated from tubers stored for two weeks under 22°C and 4°C, respectively. A
271 similar and minimal level of *VInv* expression was observed in 22°C-stored tubers from wild type
272 Katahdin and all three CRISPR/Cas lines. In contrast, the expression level of *VInv* in 4°C-stored
273 tubers of the three CRISPR/Cas lines was only 6.6%, 16.4%, and 27.3%, respectively, of the
274 wild-type Katahdin (**Figure 5G, Supplemental Table S4**). Potato chipping was performed using
275 tubers stored under 22°C and 4°C, respectively. Potato chips processed from tubers stored under
276 22°C showed a similar color from all three lines as well as wild type Katahdin (**Supplemental**

277 **Figure S7**). After the 4 weeks of storage of the tubers under 4°C, chips from KV78, KV87, and
278 KV108 all showed a lighter color than those from Katahdin (**Supplemental Figure S7**).

279 Collectively, these results showed that although the deletions associated with *VInvIn2En*
280 of Katahdin are in heterozygous and mosaic conditions in the three T0 CRISPR/Cas lines, the
281 deletions resulted in a significant reduction of *VInv* expression under cold storage condition,
282 confirming the cold-responsive function of *VInvIn2En* in Katahdin.

284 **Evolution of *VInv* gene and *VInvIn2En* enhancer**

285 We computationally extracted the DNA sequence of *VInv* gene from a total of 28
286 sequenced Solanaceous species. Sequences from several distantly related species, including *A.*
287 *thaliana*, cucumber (*Cucumis sativus*) and soybean (*Glycine max*), were used as outgroups in
288 evolutionary analysis. The VINV protein of potato shared 92-99% sequence similarity with those
289 from tomato and wild *Solanum* species (**Supplemental Figure S8**). In addition, the structure of
290 the *VInv* genes is also highly conserved among different species (**Figure 6**). The distinct small
291 exon 2 (9 bp) was detected in all Solanaceous species, as well as in several distantly related plant
292 species. In addition, a large intron 2 was identified following the small exon 2 in all species
293 (**Figure 6**), with sizes ranging from 780 bp to 2,997 bp (**Supplemental Table S5**).

294 The 1,327-bp intron 2 sequence from RH (Zhou et al., 2020) was used to align the intron
295 2 sequences from other Solanaceous species. Homologous sequences were detected in the same
296 intron of the *VInv* gene from all *Solanum* species, as well as from several distantly related
297 species, including eggplant (*Solanum melongena*) and pepper (*Capsicum annuum*)
298 (**Supplemental Table S5**). We next aligned the 200-bp *VInvIn2En* sequence from RH to the
299 intron 2 sequences from different species. Surprisingly, the *VInvIn2En* sequences were more
300 conserved than the intron 2 sequences among the species analyzed (**Supplemental Table S5**).
301 Furthermore, the DNA motifs related to CBF/NF-Y, TCP and GATA were detected in the
302 *VInvIn2En* sequences from distantly related *Solanum* species (**Supplemental Table S5**).
303 Therefore, *VInvIn2En* represents a conserved enhancer sequence in *Solanum* species.

304 We extracted the *VInvIn2En* sequence from several different potato genotypes to further
305 exploit its sequence polymorphism (**Supplemental Figure S9**), including diploid potato clones
306 M6 (Jansky et al., 2014) and H28-7 (Bhaskar et al., 2010), which are resistant to CIS. SNPs and
307 small indels were observed throughout the *VInvIn2En* sequence in comparison between CIS

308 resistant (H28-7 and M6) and CIS susceptible (RH) genotypes, including SNPs located in the
309 CBF/NF-Y, GATA and TCP motifs (**Supplemental Figure S9**). Thus, sequence polymorphism
310 of *VInvIn2En* may contribute to the level of CIS resistance of different potato genotypes.

311

312 **Discussion**

313 Invertases hydrolyze sucrose into glucose and fructose, thereby playing important roles in
314 metabolism and development in plants (Ruan et al., 2010). Different plant invertases have been
315 found to be specific to the cell wall, vacuole, or cytosol, respectively. Both cell wall and vacuolar
316 invertases are also known to contribute to defense responses to abiotic and biotic stresses (Wan
317 et al., 2018). Vacuolar invertases play essential roles in cell expansion and sugar accumulation,
318 which are related to plant growth and development (Ruan et al., 2010; Wan et al., 2018).
319 Therefore, silencing of the vacuolar invertase gene can cause major developmental defects in
320 plants. For example, silencing of the vacuolar invertase gene in tomato (*Solanum lycopersicum*)
321 resulted in substantially smaller fruits (Klann et al., 1996). Major developmental defects were
322 also reported in silencing of the vacuolar invertase gene in several other species, including carrot
323 (*Daucus carota*) (Tang et al., 1999), muskmelon (*Cucumis melo*) (Yu et al., 2008), cotton
324 (*Gossypium hirsutum*) (Wang et al., 2014; Wang and Ruan, 2016), and rice (*Oryza sativa*) (Lee
325 et al., 2019; Deng et al., 2020).

326 *VInv (Pain-1)* is the only vacuolar invertase gene identified in the potato genome
327 (Bhaskar et al., 2010; Draffehn et al., 2010). Interestingly, silencing of the *VInv* gene by RNAi in
328 potato did not cause unambiguous defects in growth and development (Bhaskar et al., 2010). The
329 potato RNAi lines did not show yield loss in field-based yield trials (Bhaskar et al., 2010). These
330 results suggest that the *VInv* gene may not play a similar developmental role in potato as
331 compared to other plant species. Although *VInv* is expressed in non-tuber tissues, the expression
332 of *VInv* is not upregulated by cold stress in several non-tuber tissues, including petiole, stem, and
333 root (X.B. Zhu, unpublished data). Similarly, the GUS signals in the transgenic *A. thaliana* plants
334 derived from *VInvIn2* and *VInvIn2En* constructs were not enhanced by cold stress. We
335 hypothesize that the *VInv* gene has adapted for a distinct role in the tuber-bearing species in
336 response to cold stress. A high level of *VInv* expression at cold temperatures would generate
337 more sugars in tuber cells, which in turn would affect the osmotic pressure and increase the
338 freezing tolerance of tuber cells that contain a high percentage of water.

339 The *VInvIn2En* sequence is conserved among distantly related *Solanum* species,
340 including tomato and several other non-tuber-bearing species (**Supplemental Table S5**,
341 **Supplemental Figure S9**). Thus, *VInvIn2En* emerged before the divergence between tuber-
342 bearing and non-tuber-bearing species. We speculate that *VInvIn2En* contains unidentified
343 sequence motif(s) that are responsible for its tuber-specific function. We previously showed that
344 the CIS-resistant diploid potato germplasm line H28-7 exhibits a very low level of *VInv*
345 expression in cold-stored tubers (Bhaskar et al., 2010). Interestingly, we detected a SNP in each
346 of the two CBF/NF-Y motifs in *VInvIn2E* between H28-7 and RH (**Supplemental Figure S9**).
347 These results suggest that variation of the *VInvIn2En* sequence is likely the key factor for the
348 resistance of the CIS-resistant germplasm. By contrast, an identical *VInvIn2En* sequence was
349 observed in DM1-3 and RH potatoes (**Supplemental Figure S9**), which have different levels of
350 resistance to CIS. Thus, the *VInv*-mediated cold tolerance is likely associated with additional
351 factors depending on species or genotypes within a species. This hypothesis is supported by
352 previous reports demonstrating an invertase inhibitor, *StInvInh2*, which specifically suppresses
353 the activity of the VINV protein (Liu et al., 2010; Brummell et al., 2011). A combination of
354 *VInvIn2En*-mediated cold-induced expression of *VInv* and post-transcriptional regulation of
355 VINV protein provide a multilayer of defense system for potato to adapt to different
356 environments and/or stress conditions.

357 Several TFs, including CBF/NF-Y, TCP, and GATA, may play a role in *VInvIn2En*-
358 mediated regulation of *VInv* under cold conditions, since mutations of the predicted binding sites
359 of these TFs abolished the function of *VInvIn2En* as a transcriptional enhancer in *A. thaliana*
360 (**Figure 3**). CBF/NF-Y, TCP, and GATA are large TF families in plants and include 41, 31, and
361 49 genes, respectively, in the potato genome (Wang et al., 2019; Li et al., 2021; Yu et al., 2022).
362 Although there are no reports yet on cold response associated with these TFs in potato, specific
363 members from the CBF/NF-Y, TCP, and GATA families have been documented for playing a
364 role in cold temperature response in other plant species. For example, a GATA-family TF in rice,
365 OsGATA16, was induced by cold treatment, and can improve cold tolerance by repressing some
366 cold-related genes (Zhang et al., 2021). A TCP1 TF in *Chrysanthemum morifolium*, DgTCP1,
367 was induced by cold temperature and can regulate peroxidase activity and reduce ROS
368 accumulation (Li et al., 2022a). It is interesting to note the presence of three CBF/NF-Y binding
369 sites in close vicinity within *VInvIn2En*. The NF-Y TFs have been documented to confer

370 response to various types of abiotic stresses, including drought, salt, nutrient and temperature
371 (Zhang et al., 2023). Thus, it will be essential to validate the functions of these TF-binding sites
372 in potato and to identify a specific member(s) from these TF families that are responsible for the
373 function of *VInvIn2En*.
374

375 **Materials and Methods**

376 **Enhancer validation using transgenic assays in potato**

377 An intronic DHS within intron 2 of *VInv* gene was identified from the DHS data
378 published previously (Zeng et al., 2019). The entire intron 2 from the *VInv* gene of RH potato
379 (*Solanum tuberosum*) was used for enhancer validation using a GUS reporter system (Zhu et al.,
380 2015). The forward (*VInvIn2*) and reverse (*VInvIn2R*) sequences of intron 2 were amplified from
381 genomic DNA of RH potato using PCR with primers VIT-F6/R6 and VIT-F8/R8 (**Supplemental**
382 **Table S3**), respectively, and were ligated to a minimal 35S promoter (-50 to -2 bp) (m35S)
383 through the *EcoRI* cloning site. The ligated PCR products were cloned into the pENTR/D
384 directional TOPO cloning vector (Invitrogen) and then transferred into the pKGWFS 7.0 vector
385 containing the GUS reporter using the LR Clonase recombination method (Zhu et al., 2015).
386 Constructs were transferred into *Agrobacterium tumefaciens* strain GV3101 (pMP90), followed
387 by transformation to potato variety Katahdin using methods described previously (Bhaskar et al.,
388 2008; Bhaskar et al., 2010).

389 Transgenic Katahdin lines derived from the forward or reverse construct were obtained
390 and screened using PCR with the kanamycin gene-specific primers Kan-F/R and the construct-
391 specific primers (**Supplemental Table S3**). All transgenic lines with three replicates for each line
392 were grown in greenhouses using photoperiod of 16-h daylight at 22°C and 8-h darkness at 16°C
393 (50%-70% humidity), and light intensity of 500 $\mu\text{mol m}^{-2} \text{s}^{-1}$ (natural light combined with light of
394 high-pressure sodium lamps) until leaves became senesced naturally. Tubers harvested from each
395 line were divided into two groups: stored in dark at 22°C (50%-70% humidity) or 4°C (60%-70%
396 humidity) for 4 weeks, respectively. Tuber slices prepared by slicing longitudinal sections 2-mm
397 thick from the center of individual tubers were examined for GUS activity. Tuber slices were
398 placed in a plastic plate (70 x 15 mm) and soaked in GUS-staining solution (100 mM sodium
399 phosphate, pH 7.0, 10 mM EDTA, 0.1% [v/v] Triton X-100, 0.5 mM potassium ferrocyanide, 0.5
400 mM potassium ferricyanide, and 0.05% [w/v] X-Gluc), with vacuum infiltration for 30 min and

401 incubation in dark at 37°C overnight. Tuber slices were washed in 80% (v/v) ethanol several
402 times. Images of tuber slices were captured using an EPSON Perfection 4180 scanner.

403

404 **Enhancer dissection using transgenic assays in *A. thaliana***

405 Seeds of *Arabidopsis* (*Arabidopsis thaliana*) accession Col-0 were germinated in one-
406 half-strength Murashige and Skoog (0.5 x MS) medium, and the seedlings were transplanted in
407 potting soil and grown in plant growth chambers with 16/8 h light/dark cycles at 23°C and light
408 intensity of 150 $\mu\text{mol m}^{-2} \text{s}^{-1}$ (white fluorescent lamps) until flowering. The *VInvIn2* and
409 *VInvIn2R* constructs were initially used to transform *A. thaliana* accession Col-0 using the
410 floral dip method (Clough and Bent, 1998). Transgenic seedlings were screened on solid 0.5 x
411 MS medium containing kanamycin (50 $\mu\text{g mL}^{-1}$) and were grown in an illumination incubator
412 with the same light-dark condition described above and were examined for GUS activity
413 according to published protocols (Zhu et al., 2015).

414 To map the position of the enhancer within the intron 2 of *VInv*, we divided the intron 2
415 into ten DNA fragments (#1 to #10) using five breaks (b1 to b5) for transgenic assays. The
416 stem/petiole-specific enhancer (within DNA fragment #11) was further divided into 14 (#11 to
417 #24) sub-fragments. All target DNA fragments together with the m35S were synthesized from
418 GenScript Inc. and cloned into the pKGWFS 7.0 vector containing the m35S and the *GUS*
419 reporter gene (Zhu et al., 2015). Images of transgenic *A. thaliana* seedlings were captured using
420 the EPSON Perfection 4180 scanner to record the GUS signals.

421

422 **Analysis of TF-binding motifs**

423 TF-binding motifs and their corresponding TFs within intron 2 of *VInv* were identified
424 using two independent programs of CIS-BP (Weirauch et al., 2014) and PlantPAN 3.0 (Chow et
425 al., 2019) with default parameters. DNA motifs consistently detected by both programs were
426 used for further analysis. Motifs reported to be associated with cold response in one or multiple
427 plant species were mapped to the intron 2 of *VInv* using TBtools (Chen et al., 2020).

428

429 **Development of CRISPR/Cas deletion lines**

430 A self-compatible diploid potato clone DMF5-73-1 was developed from a cross between
431 *S. tuberosum* Gp. Phureja DM 1-3 516 R44 (DM1-3) and *Solanum chacoense* (M6) (Endelman

432 and Jansky, 2016) and has been self-pollinated for five generations. Wild type (WT) and
433 CRISPR/Cas lines were propagated *in vitro* on Murashige and Skoog (MS) medium (MS basal
434 salts plus vitamins, 3% sucrose, 0.7% plant agar, pH 5.8) (Murashige and Skoog, 1962). *In vitro*
435 plants were maintained in growth chambers with 16-h-light/8-h-dark photoperiod at 22°C and
436 average light intensity of 200 $\mu\text{mol m}^{-2} \text{s}^{-1}$ (white fluorescent lamps) *Pro*.

437 The Csy4-based CRISPR/Cas9 system (Cermak et al., 2017) was used to develop
438 *VInvIn2En* deletion lines in DMF5-73-1. In brief, five sgRNAs flanking *VInvIn2En* (1a, 2a, 3a,
439 1b and 2b) and a single sgRNA (3b) targeting *VInvIn2En* (**Supplemental Table S2**) were
440 designed using program of CRISPR-P v2.0 (Liu et al., 2017). The six gRNAs were linked by
441 Csy4 binding sites and then cloned into the Csy4 multiplexing vector (**Supplemental Figure S3**)
442 based on published methods (Cermak et al., 2017). The construct was delivered into *A.*
443 *tumefaciens* GV3101 (pMP90) and was used to conduct hairy root-based *Agrobacterium*
444 transformation (Butler et al., 2020). T0 CRISPR/Cas lines showing the expected smaller PCR
445 products were further confirmed by Sanger sequencing using *VInv*-mut-F1/R1 primers
446 (**Supplemental Table S3**). Several T0 lines with large deletion of *VInvIn2En* were grown under
447 greenhouse conditions as described above, followed by subsequent self-pollination to obtain
448 homozygous T1 deletion lines.

449 A tetraploid potato cultivar Katahdin was used to develop deletion lines using the U3/U6-
450 based CRISPR/Cas9 system (Hu et al., 2019). Four sgRNAs, including R1 outside of *VInvIn2En*,
451 and R2, R3, and R4 inside the *VInvIn2En* (**Supplemental Table S2**), were designed using
452 CRISPR-P v2.0 (Liu et al., 2017). The sgRNAs were assembled into four expression cassettes
453 (*ProAtU3b:gRNA1*, *ProAtU3d:gRNA2*, *ProAtU6-29:gRNA3*, and *ProAtU6-29:gRNA4*), which
454 were cloned into the pHNCas9 vector by using the Golden Gate cloning strategy (Ma et al., 2015;
455 Xie et al., 2015; Ma et al., 2016; Hu et al., 2019). The construct pHNCas9::*VInvIn2En* was
456 introduced into *A. tumefaciens* GV3101 (pMP90) and was used to transform Katahdin according
457 to published protocols (Bhaskar et al., 2008). Positive transformants were screened using PCR
458 with primers *Kan*-F3/R3, *Cas*-F1/R1, and *VInv*-Edit-F/R (**Supplemental Table S3**). Transgenic
459 lines containing additional smaller bands (2% agarose gel) were further confirmed by Sanger
460 sequencing. PCR products were purified by using QIAquick PCR Purification Kit (Qiagen) and
461 were cloned into *Escherichia coli* using pMDTM19-T vector (TaKaRa). A minimum of 60
462 randomly selected positive colonies derived from each deletion line were fully sequenced.

463 Statistical analysis of different types of deletions was conducted on each of the Katahdin
464 CRISPR/Cas deletion lines containing three haplotypes, A (2 copies), B, and C.

465

466 **Greenhouse trials, tuber sample preparation, and chipping analysis**

467 Each of 10 seed tubers of RH potato was planted in potting soil under normal greenhouse
468 conditions as described above. Standard cultivation and management practices were followed
469 throughout the growing period. Tubers were harvested 120 days after seedling emergence when
470 leaves senesced naturally. Tubers harvested from two pots were combined together as one
471 biological replicate. Tubers of five biological replicates were stored in dark at 22°C (50%-70%
472 humidity) for 10 days and then divided into two groups. Each group was stored in dark at 22°C
473 (50%-70% humidity) or 4°C (60%-70% humidity) for 0, 2, 4, 8, and 16 weeks, respectively.

474 Three T0 CRISPR/Cas deletion lines (three plants for each line) developed from
475 Katahdin were grown under normal greenhouse conditions as described above. Tubers harvested
476 from the same line were combined together and stored under dark at 22°C for 10 days, and then
477 divided into two groups for 22°C (50%-70% humidity) or 4°C (60%-70% humidity) treatments,
478 and each group of tubers with three replicates were treated for 2 and 4 weeks, respectively.

479 Tuber samples of 1.5-mm thick slices (1-3 slices for each tuber) prepared from apical to
480 basal end of the tuber were taken for chipping analysis. The remaining tuber samples were frozen
481 in liquid nitrogen and used for analysis of *VInv* expression. Tuber slices were fried in cottonseed
482 oil at 191°C for 2 min or until the cessation of bubbles. Chip color of cold-stored tubers is
483 compared to that of the corresponding controls.

484

485 ***VInv* transcription and splicing assays**

486 RNAs were extracted from tuber tissues using Plant RNA Isolation Mini Kit (Agilent)
487 following the manufacturer's instructions and were reverse transcribed to cDNAs using
488 Invitrogen SuperScript™ III Reverse Transcriptase Kit (Invitrogen) with oligo(dT)₂₀ primer.
489 *VInv* transcripts were quantified by reverse transcription quantitative PCR (RT-qPCR) using the
490 SYBR Advantage qPCR Premix (Clontech) with the specific primers for *VInv* and the reference
491 gene *Actin97* described previously (Zhu et al., 2014; Zhu et al., 2016). RT-qPCR was performed
492 on the CFX96 Touch™ Real-Time PCR Detection System (Bio-Rad) with a program of 30 s at
493 95°C, 40 cycles of 10 s at 95°C, 20 s at 60°C for *VInv* and *Actin97*, and 30 s at 72°C, followed

494 by a plate read. Then 2 s at 50°C to 95°C with 0.2°C steps for melting curve, followed by a final
495 extension step of 10 min at 72°C. Relative expression levels of *VInv* gene were calculated using
496 Gene Expression Macro software version 1.1 (Bio-Rad Laboratories). Data for each treatment
497 are presented as standard error (SE) of means of the three biological replicates. For RT-qPCR
498 data of three Katahdin CRISPR/Cas9 lines and the wild type, analyses of variance (ANOVA)
499 were carried out using PROC GLM in the Statistical Analysis System version 9.1 (SAS v9.1)
500 (SAS Institute Inc, Cary, NC) (**Supplemental Table S4**).

501 To examine whether *VInvIn2En* deletions affect *VInv* gene splicing, we prepared cDNAs
502 from tuber tissues of the three Katahdin CRISPR/Cas lines. Exon 1 to exon 3 of *VInv* was
503 amplified using primers Splicing-F/R (**Supplemental Table S3**, amplicon size: 612 bp). The RT-
504 PCR products were purified by using QIAquick PCR Purification Kit (Qiagen) and then used for
505 Sanger sequencing.

506

507 **Yeast one-hybrid (Y1H) assay**

508 Triple copies of the *VInvIn2En* sequence (*VInvIn2En**3) were synthesized and used to
509 develop a bait plasmid p*VInvIn2En**3-AbAi. The bait plasmid was used to screen the cDNA
510 library, developed from cold-treated tuber tissues of RH potato, according to methods described
511 in the Matchmaker[®] Gold Yeast One-Hybrid Library Screening System User Manual (Clontech,
512 <http://www.takarabio.com/>). Yeast (*Saccharomyces cerevisiae*) colonies were cultured on plates
513 containing SD/-Leu/AbA^{200 ng/mL} medium at 30°C for 3-5 days, and those greater than 2 mm in
514 diameter were analyzed by PCR amplification and Sanger sequencing using primers pGADT7-
515 F/R (**Supplemental Table S3**). The resulted sequences from the 387 yeast colonies were used
516 for BLAST search in the DM1-3 potato cDNA (v6.1) database by using Spud DB blastn program
517 with default parameters (<http://spuddb.uga.edu/blast.shtml>). We identified the best matched
518 cDNA sequence for each of the 387 sequences. The cDNA sequences with an E-value <1e-5 and
519 a minimum sequence identity of 82% were kept for further analyses. We identified a total of 33
520 unique cDNA sequences after filtering out repetitive cDNA sequences.

521 To further validate the interactions between the candidate proteins and the *VInvIn2En*
522 enhancer, point-to-point Y1H assay was performed. Full-length CDSs of the candidate proteins
523 related to the 33 identified cDNAs were inserted into the prey vector pGADT7 by using HB-
524 infusion[™] Cloning Kit (HANBIO, <https://www.hanbio.net/en/company.shtml/>). The prey

525 plasmids were subsequently transformed into the bait yeast strain Y1HGold[p*VInvIn2En**3-
526 AbAi] by using the Yeastmaker™ Yeast Transformation System 2 (Clontech,
527 <http://www.takarabio.com/>). The yeast colonies were transferred to plates containing SD/-
528 Leu/AbA^{200 ng/mL} medium and then allowed to grow at 30°C for 3 days.

530 **Analysis of *VInv* evolution**

531 A total of 28 Solanaceous species (<https://solgenomics.net/>) (Tang et al., 2022) and
532 several other dicot species (**Supplemental Table S5**), including *A. thaliana*, cucumber (*Cucumis*
533 *sativus*), and soybean (*Glycine max*), were selected for evolutionary analysis of the *VInv* gene.
534 Information on evolutionary timescale of life for all 31 species were collected from the TimeTree
535 5 database (<http://www.timetree.org/>) (Kumar et al., 2022) and visualized in MEGA X software
536 (Kumar et al., 2018).

537 Protein sequences of *VInv* gene from the 31 different plant species were extracted and
538 aligned to that from RH potato using the NCBI BLASTp program
539 (<https://blast.ncbi.nlm.nih.gov/Blast.cgi>). The intron and exon composition of the *VInv* gene from
540 31 plant species were analyzed using the online tool GSDS 2.0 (Hu et al., 2015). The 1327-bp
541 intron 2 and the 200-bp *VInvIn2En* sequences from RH were used to align the intron 2 sequences
542 from other 30 species to identify homologous sequences using program of NCBI BLASTn.

544 **Accession Numbers**

545 Sequence data from this article can be found in the GenBank/EMBL libraries under the
546 following accession numbers: Soltu.DM.03G015280 (*VInv*), Soltu.DM.01G024340 (StNF-YC9),
547 and Soltu.DM.06G027230 (StNF-YC1). All mutants and transgenic lines are described in

548 **Supplemental Table S6.**

549
550
551
552
553
554
555

556
557
558
559
560
561
562
563
564
565
566
567
568
569
570
571
572
573
574
575

576 **Funding information**

577 Research was supported by grant 31771857 from the National Natural Science Foundation of
578 China, grant 1808085MC65 from Anhui Provincial Natural Science Foundation, grant 2021H276
579 from the Scientific Research Fund for Candidates of Anhui Provincial Academic and Technical
580 Leaders, and grant 22532002 from Anhui Province Vegetable Industry Technology System Fund
581 to X.Z.; by USDA-NIFA-SCRI grant 2011-51181-30629 to J.J.; by grants IS-5038-17C and IS-
582 5317-20C from BARD (the United States - Israel Binational Agricultural Research and
583 Development Fund) to D.E. and J.J.; and by AgBioResearch at Michigan State University (Hatch
584 grant MICL02571) and MSU startup fund to J.J.

585

586 **Acknowledgments**

587 This research project was initiated at the University of Wisconsin-Madison and continued by
588 Zhu lab at Anhui Agricultural University and Jiang lab at Michigan State University. We are
589 grateful to Dr. Hainan Zhao (China Agricultural University) for assistance on evolutionary
590 analysis of *VInv* gene and to Dr. Nan Hu (Anyang Institute of Technology) for providing the
591 U3/U6-based CRISPR/Cas9 genome-editing system (the pHNCas9 binary vector).

592

593 **Availability of data and materials**

594 All materials, including constructs, are available upon request.

595 **Author contributions**

596 J.J. conceived the research. X.Z., A.C., N.M.B. and J.J. designed the experiments. X.Z., A.C.,
597 N.M.B., Z.Z., H.X., L.W., and Z.L. conducted the experiments. X.Z., D.E., D.S.D., and J.J.
598 analyzed the data. X.Z. and J.J. wrote the manuscript.

599

600 **Competing interests**

601 The authors declare no competing interests.

602

603 **Figure legends**

604 **Figure 1.** Discovery of a cold-responsive intronic enhancer in *VInv* gene. (A) DNase-
605 hypersensitive sites (DHSs) associated with *VInv* gene. DHS map was developed from tuber
606 tissue of DM1-3 potato. Two DHSs (red bars), one at the 5' of the gene and one in the second
607 intron, were detected. (B) β -glucuronidase (GUS) reporter gene assays of the second intron of
608 *VInv* gene in Katahdin potato. Constructs using a minimal 35S promoter (m35S) and a full-
609 length 35S promoters were used as negative and positive controls. Tubers from transgenic
610 Katahdin lines developed using the intronic construct (*VInvIn2*) and a reverse construct
611 (*VInvIn2R*) showed minimal GUS signals under room temperature (22°C). Strong GUS signals
612 were detected from tubers after 4 weeks of cold storage under 4°C. The scale bar represent 2 cm.

613

614 **Figure 2.** Identification of transcriptional enhancers in intron 2 of *VInv* gene. (A) A diagram
615 illustrating the sizes and positions of 10 sub-fragments derived from intron 2 of the *VInv* gene.

616 The 1327-bp intron was divided into ten fragments (#1 to #10) using five breaks (b1 to b5). **(B)**
617 β -glucuronidase (GUS) reporter gene assays of the intron 2 in *A. thaliana*. Constructs with
618 minimal 35S promoter (m35S) and a full-length 35S promoter (35S) were used as negative and
619 positive controls. **(C)** GUS expression patterns of representative *A. thaliana* transgenic seedlings
620 derived from each of the ten constructs consisting of a fragment ligated with the m35S promoter
621 and the GUS reporter gene. **(D)** A diagram illustrating the sizes and positions of the 13 fragments
622 derived from the DNA fragment #11. A dashed red line marks the middle point of the 600-bp
623 segment #11. “+” and “-” indicate the derived transgenic seedlings showing positive and
624 negative GUS signals, respectively. **(E)** GUS staining of 20 *A. thaliana* transgenic seedlings
625 derived from constructs #11, #17, #19, and #21, respectively. **(F)** GUS reporter gene assay of the
626 200-bp *VInvIn2En* enhancer in Katahdin potato. Tubers from three independent transgenic lines
627 showed minimal GUS signals under 22°C but strong signals from tubers after 4 weeks of cold
628 storage under 4°C. All numbers above bars/lines in (A) and (D) indicate base pairs. The scale bar
629 represents 2 mm in (B, C) and 1 cm in (E, F). Fragment numbers highlighted in red color in (A,
630 C, D, E) indicate representative constructs with full enhancer function.

631
632 **Figure 3.** Distribution and function of DNA motifs in intron 2 and the *VInvIn2En* enhancer. **(A)**
633 Distribution of DNA motifs related to transcription factors (TFs) involved in response to cold
634 stress. Each vertical bar represents a potential TF-binding site. A red horizontal bar marks the
635 position of the 200-bp enhancer. Vertical blue bars indicate that the binding sites of a relevant TF
636 are enriched or exclusively located within the 200-bp enhancer. Vertical green bars indicate that
637 the binding sites of a relevant TF are not enriched within the enhancer **(B)** Transgenic assays of
638 *VInvIn2En* with mutated DNA motifs related to five different TFs. Red colored nucleotides
639 indicate the replaced sequence(s) in each construct. No β -glucuronidase (GUS) signals were
640 detected in any transgenic *A. thaliana* plants derived from the three constructs with mutated
641 motifs related to CBF/NF-Y, TCP, and GATA.

642
643 **Figure 4.** Identification of StNF-YC1 and StNF-YC9 proteins that bind to *VInvIn2En* using yeast
644 one-hybrid assay. Triple copies of the *VInvIn2En* sequence (*VInvIn2En**3) were synthesized to
645 develop the bait plasmid p*VInvIn2En**3-AbAi. The pGADT7 vector was used as negative control,

646 and a combination of two constructs (p53-AbAi and pGADT7-Rec-p53) was used as positive
647 control.

648

649 **Figure 5.** Functional validation of the *VInvIn2En* enhancer using genome editing. **(A)** A diagram
650 illustrating the positions of all sgRNAs within and outside of intron 2 of *VInv* gene. The red bar
651 marks the 200-bp enhancer *VInvIn2En*. Red arrows indicate the position of sgRNAs R1, R2, R3,
652 and R4. Blue arrows indicate the position of sgRNAs 1a, 2a, 3a, 1b, 2b, and 3b. **(B)** Gel
653 electrophoresis of PCR products amplified from the three homozygous CRISPR/Cas9 deletion
654 lines (2-2-8, 13-1-3 and 13-2-1) developed from the wild-type (WT) DMF5-73-1. **(C)** Reverse
655 transcription quantitative PCR (RT-qPCR)-based transcription analysis of *VInv* gene in cold-
656 stored potato tissues from the three homozygous deletion lines (2-2-8, 13-1-3 and 13-2-1). All
657 three lines showed significant reduction of *VInv* expression relative to the *Actin97* reference gene.
658 The y axis represents the relative expression level normalized by setting *VInv* expression in cold-
659 stored tubers of the wild-type (WT) DMF5-73-1 to 1. Data is presented as mean \pm standard
660 deviation (SD) from three biological replicates and was tested by the Student *t*-test ($*P < 0.05$).
661 **(D)** Chipping of tubers from deletion line 13-1-3 and from the WT DMF5-73-1. Note: (1) the
662 dark color toward one end of each chip is caused by the “jelly end” problem (two examples are
663 indicated by arrows) associated with both 13-1-3 and WT. (2) 13-1-3 is a selfed progeny of a T0
664 DMF5-73-1 (heterozygous) transgenic line. Thus, the tubers from the two lines show different
665 shapes. Three tubers from each line were used for chipping, and two chips from each tuber were
666 included in the illustration. **(E)** Gel electrophoresis of PCR products amplified from the genomic
667 DNA of three T0 CRISPR/Cas9 lines (KV78, KV87 and KV108) developed from tetraploid
668 potato cultivar Katahdin. Red arrows indicate fragments resulted from deletions within
669 *VInvIn2En*. **(F)** Sequencing of PCR products amplified from cDNAs of the three CRISPR/Cas9
670 lines. Normal splicing between exon 1 and exon 3 was detected in all three lines. **(G)** Reverse
671 transcription quantitative (RT-qPCR)-based analysis of *VInv* expression relative to the *Actin97*
672 gene of the three CRISPR/Cas lines. Expression was analyzed using tubers after 2 weeks of
673 storage at 22°C and 4°C, respectively. The y axis represents the relative expression level
674 normalized by setting *VInv* expression in 22°C-stored tubers of the wild-type Katahdin to 1. Data
675 is presented as mean \pm standard deviation (SD) from three biological replicates and were tested

676 by using PROC GLM analyses of variance (ANOVA). Different lower case letters represent
677 statistically significant differences at P = 0.05.

678

679 **Figure 6.** Composition of introns and exons of *VInv* genes from different plant species. A total of
680 28 Solanaceous species and eight distantly related dicot species were selected for the analysis.
681 The distinctly small exon 2 (9 bp) was detected in all Solanaceous species, as well as in five
682 distantly related plant species. In addition, a large intron 2 (ranging from 780 bp to 2,997 bp)
683 following the small exon 2, was identified in most plant species

684

685

686

687

688 **References**

- 689 **Agarwal, S., Chakrabarti, S.K., Shikha, M., Chimote, V.P., Pattanayak, D., and Naik, P.S.**
690 (2003). A biotechnological approach for reduction of cold-induced sweetening in potato
691 tubers. *J. Indian Potato Assoc.* **30**, 39-40.
- 692 **Amrein, T.M., Bachmann, S., Noti, A., Biedermann, M., Barbosa, M.F., Biedermann-Brem,**
693 **S., Grob, K., Keiser, A., Realini, P., Escher, F., and Amado, R.** (2003). Potential of
694 acrylamide formation, sugars, and free asparagine in potatoes: A comparison of cultivars
695 and farming systems. *J. Agric. Food Chem.* **51**, 5556-5560.
- 696 **Bagnaresi, P., Moschella, A., Beretta, O., Vitulli, F., Ranalli, P., and Perata, P.** (2008).
697 Heterologous microarray experiments allow the identification of the early events
698 associated with potato tuber cold sweetening. *BMC Genomics* **9**, 176.
- 699 **Becalski, A., Lau, B.P.Y., Lewis, D., Seaman, S.W., Hayward, S., Sahagian, M., Ramesh,**
700 **M., and Leclerc, Y.** (2004). Acrylamide in french fries: Influence of free amino acids
701 and sugars. *J. Agric. Food Chem.* **52**, 3801-3806.
- 702 **Bhaskar, P.B., Raasch, J.A., Kramer, L.C., Neumann, P., Wielgus, S.M., Austin-Phillips, S.,**
703 **and Jiang, J.M.** (2008). *Sgt1*, but not *Rar1*, is essential for the *RB*-mediated broad-
704 spectrum resistance to potato late blight. *BMC Plant Biol.* **8**, 8.
- 705 **Bhaskar, P.B., Wu, L., Busse, J.S., Whitty, B.R., Hamernik, A.J., Jansky, S.H., Buell, C.R.,**
706 **Bethke, P.C., and Jiang, J.M.** (2010). Suppression of the vacuolar invertase gene
707 prevents cold-induced sweetening in potato. *Plant Physiol.* **154**, 939-948.
- 708 **Braun, S.R., Endelman, J.B., Haynes, K.G., and Jansky, S.H.** (2017). Quantitative trait loci
709 for resistance to common scab and cold-induced sweetening in diploid potato. *Plant*
710 *Genome* **10**, DOI: 10.3835/plantgenome2016.3810.0110.
- 711 **Brummell, D.A., Chen, R.K.Y., Harris, J.C., Zhang, H.B., Hamiaux, C., Kralicek, A.V.,**
712 **and McKenzie, M.J.** (2011). Induction of vacuolar invertase inhibitor mRNA in potato
713 tubers contributes to cold-induced sweetening resistance and includes spliced hybrid
714 mRNA variants. *J Exp Bot* **62**, 3519-3534.

- 715 **Butler, N.M., Jansky, S.H., and Jiang, J.M.** (2020). First-generation genome editing in potato
716 using hairy root transformation. *Plant Biotechnol J* **18**, 2201-2209.
- 717 **Byrne, S., Meade, F., Mesiti, F., Griffin, D., Kennedy, C., and Milbourne, D.** (2020).
718 Genome-wide association and genomic prediction for fry color in potato. *Agronomy-*
719 *Basel* **10**, 90.
- 720 **Cermak, T., Curtin, S.J., Gil-Humanes, J., Cegan, R., Kono, T.J.Y., Konecna, E., Belanto,**
721 **J.J., Starker, C.G., Mathre, J.W., Greenstein, R.L., and Voytasa, D.F.** (2017). A
722 multipurpose toolkit to enable advanced genome engineering in plants. *Plant Cell* **29**,
723 1196-1217.
- 724 **Chen, C.J., Chen, H., Zhang, Y., Thomas, H.R., Frank, M.H., He, Y.H., and Xia, R.** (2020).
725 TBtools: an integrative toolkit developed for interactive analyses of big biological data.
726 *Mol Plant* **13**, 1194-1202.
- 727 **Chen, R.G., Ma, J.H., Luo, D., Hou, X.M., Ma, F., Zhang, Y.M., Meng, Y.C., Zhang, H.F.,**
728 **and Guo, W.L.** (2019). CaMADS, a MADS-box transcription factor from pepper, plays
729 an important role in the response to cold, salt, and osmotic stress. *Plant Sci* **280**, 164-174.
- 730 **Chow, C.N., Lee, T.Y., Hung, Y.C., Li, G.Z., Tseng, K.C., Liu, Y.H., Kuo, P.L., Zheng,**
731 **H.Q., and Chang, W.C.** (2019). PlantPAN3.0: a new and updated resource for
732 reconstructing transcriptional regulatory networks from ChIP-seq experiments in plants.
733 *Nucleic Acids Res* **47**, D1155-D1163.
- 734 **Clasen, B.M., Stoddard, T.J., Luo, S., Demorest, Z.L., Li, J., Cedrone, F., Tibebe, R.,**
735 **Davison, S., Ray, E.E., Daulhac, A., Coffman, A., Yabandith, A., Retterath, A.,**
736 **Haun, W., Baltes, N.J., Mathis, L., Voytas, D.F., and Zhang, F.** (2016). Improving
737 cold storage and processing traits in potato through targeted gene knockout. *Plant*
738 *Biotechnol J* **14**, 169-176.
- 739 **Clough, S.J., and Bent, A.F.** (1998). Floral dip: a simplified method for *Agrobacterium-*
740 mediated transformation of *Arabidopsis thaliana*. *Plant J.* **16**, 735-743.
- 741 **Dahro, B., Wang, Y., Khan, M., Zhang, Y., Fang, T., Ming, R.H., Li, C.L., and Liu, J.H.**
742 (2022). Two AT-Hook proteins regulate A/NINV7 expression to modulate sucrose
743 catabolism for cold tolerance in *Poncirus trifoliata*. *New Phytol* **235**, 2331-2349.
- 744 **Dale, M.F.B., and Bradshaw, J.E.** (2003). Progress in improving processing attributes in potato.
745 *Trends Plant Sci* **8**, 310-312.
- 746 **Deng, X.S., Han, X.H., Yu, S.C., Liu, Z.J., Guo, D.M., He, Y., Li, W.Y., Tao, Y., Sun, C.W.,**
747 **Xu, P.Z., Liao, Y.X., Chen, X.Q., Zhang, H.Y., and Wu, X.J.** (2020). *OsINV3* and its
748 homolog, *OsINV2*, control grain size in rice. *Int J Mol Sci* **21**, 2199.
- 749 **Devaux, A., Goffart, J.-P., Petsakos, A., Kromann, P., Gatto, M., Okello, J., Suarez, V., and**
750 **Hareau, G.** (2020). Global food security, contributions from sustainable potato agri-food
751 systems. In *The potato crop: its agricultural, nutritional and social contribution to*
752 *humankind*, H. Campos, Ortiz, O., ed (Dordrecht: Springer), pp. 3-35.
- 753 **Draffehn, A.M., Meller, S., Li, L., and Gebhardt, C.** (2010). Natural diversity of potato
754 (*Solanum tuberosum*) invertases. *BMC Plant Biology* **10**, 271.
- 755 **Endelman, J.B., and Jansky, S.H.** (2016). Genetic mapping with an inbred line-derived F2
756 population in potato. *Theor Appl Genet* **129**, 935-943.
- 757 **Fang, C., Yang, M.Y., Tang, Y.C., Zhang, L., Zhao, H.N., Ni, H.J., Chen, Q.S., Meng, F.L.,**
758 **and Jiang, J.M.** (2023). Dynamics of *cis*-regulatory sequences and transcriptional
759 divergence of duplicated genes in soybean. *Proc Natl Acad Sci U S A* **120**, e2303836120.

- 760 **Fischer, M., Schreiber, L., Colby, T., Kuckenberg, M., Tacke, E., Hofferbert, H.R.,**
761 **Schmidt, J., and Gebhardt, C.** (2013). Novel candidate genes influencing natural
762 variation in potato tuber cold sweetening identified by comparative proteomics and
763 association mapping. *Bmc Plant Biology* **13**, 113.
- 764 **Greiner, S., Rausch, T., Sonnewald, U., and Herbers, K.** (1999). Ectopic expression of a
765 tobacco invertase inhibitor homolog prevents cold-induced sweetening of potato tubers.
766 *Nat. Biotech.* **17**, 708-711.
- 767 **He, F., Li, H.G., Wang, J.J., Su, Y.Y., Wang, H.L., Feng, C.H., Yang, Y.L., Niu, M.X., Liu,**
768 **C., Yin, W.L., and Xia, X.L.** (2019). PeSTZ1, a C2H2-type zinc finger transcription
769 factor from *Populus euphratica*, enhances freezing tolerance through modulation of ROS
770 scavenging by directly regulating PeAPX2. *Plant Biotechnol J* **17**, 2169-2183.
- 771 **Hu, B., Jin, J.P., Guo, A.Y., Zhang, H., Luo, J.C., and Gao, G.** (2015). GSDS 2.0: an
772 upgraded gene feature visualization server. *Bioinformatics* **31**, 1296-1297.
- 773 **Hu, N., Xian, Z.Q., Li, N., Liu, Y.D., Huang, W., Yan, F., Su, D.D., Chen, J.X., and Li, Z.G.**
774 (2019). Rapid and user-friendly open-source CRISPR/Cas9 system for single- or multi-
775 site editing of tomato genome. *Hortic Res-England* **6**, 7.
- 776 **Jansky, S.H., Chung, Y.S., and Kittipadukal, P.** (2014). M6: A diploid potato inbred line for
777 use in breeding and genetics research. *Journal of Plant Registrations* **8**, 195-199.
- 778 **Jiang, J.M.** (2015). The 'dark matter' in the plant genomes: non-coding and unannotated DNA
779 sequences associated with open chromatin. *Curr Opin Plant Biol* **24**, 17-23.
- 780 **Klann, E.M., Hall, B., and Bennett, A.B.** (1996). Antisense acid invertase (TIV1) gene alters
781 soluble sugar composition and size in transgenic tomato fruit. *Plant Physiol.* **112**, 1321-
782 1330.
- 783 **Kumar, S., Stecher, G., Li, M., Knyaz, C., and Tamura, K.** (2018). MEGA X: molecular
784 evolutionary genetics analysis across computing platforms. *Molecular Biology and*
785 *Evolution* **35**, 1547-1549.
- 786 **Kumar, S., Suleski, M., Craig, J.M., Kaspruwicz, A.E., Sanderford, M., Li, M., Stecher, G.,**
787 **and Hedges, S.B.** (2022). TimeTree 5: an expanded resource for species divergence
788 times. *Molecular Biology and Evolution* **39**, msac174.
- 789 **Lee, D.W., Lee, S.K., Rahman, M.M., Kim, Y.J., Zhang, D.B., and Jeon, J.S.** (2019). The
790 role of rice vacuolar invertase2 in seed size control. *Molecules and Cells* **42**, 711-720.
- 791 **Li, L., Paulo, M.J., Strahwald, J., Lubeck, J., Hofferbert, H.R., Tacke, E., Junghans, H.,**
792 **Wunder, J., Draffehn, A., van Eeuwijk, F., and Gebhardt, C.** (2008). Natural DNA
793 variation at candidate loci is associated with potato chip color, tuber starch content, yield
794 and starch yield. *Theor. Appl. Genet.* **116**, 1167-1181.
- 795 **Li, S.G., Zhang, N., Zhu, X., Ma, R., Liu, S.Y., Wang, X., Yang, J.W., and Si, H.J.** (2021).
796 Genome-wide analysis of *NF-Y* genes in potato and functional identification of *StNF-YC9*
797 in drought tolerance. *Front Plant Sci* **12**, 749688
- 798 **Li, X., Yang, Q., Liao, X.Q., Tian, Y.C., Zhang, F., Zhang, L., and Liu, Q.L.** (2022a). A
799 natural antisense RNA improves chrysanthemum cold tolerance by regulating the
800 transcription factor DgTCP1. *Plant Physiol* **190**, 605-620.
- 801 **Li, X.D., Zhuang, K.Y., Liu, Z.M., Yang, D.Y., Ma, N.N., and Meng, Q.W.** (2016).
802 Overexpression of a novel NAC-type tomato transcription factor, SINAM1, enhances the
803 chilling stress tolerance of transgenic tobacco. *J Plant Physiol* **204**, 54-65.

- 804 **Li, Z.Y., Fu, D.Y., Wang, X., Zeng, R., Zhang, X., Tian, J.G., Zhang, S.S., Yang, X.H., Tian,**
805 **F., Lai, J.S., Shi, Y.T., and Yang, S.H.** (2022b). The transcription factor bZIP68
806 negatively regulates cold tolerance in maize. *Plant Cell* **34**, 2833-2851.
- 807 **Liu, C.T., Ou, S.J., Mao, B.G., Tang, J.Y., Wang, W., Wang, H.R., Cao, S.Y., Schlappi,**
808 **M.R., Zhao, B.R., Xiao, G.Y., Wang, X.P., and Chu, C.C.** (2018). Early selection of
809 bZIP73 facilitated adaptation of japonica rice to cold climates. *Nat Commun* **9**, 3302.
- 810 **Liu, H., Ding, Y.D., Zhou, Y.Q., Jin, W.Q., Xie, K.B., and Chen, L.L.** (2017). CRISPR-P 2.0:
811 an improved CRISPR-Cas9 tool for genome editing in plants. *Mol Plant* **10**, 530-532.
- 812 **Liu, X., Song, B.T., Zhang, H.L., Li, X.Q., Xie, C.H., and Liu, J.** (2010). Cloning and
813 molecular characterization of putative invertase inhibitor genes and their possible
814 contributions to cold-induced sweetening of potato tubers. *Mol Genet Genomics* **284**,
815 147-159.
- 816 **Liu, X., Zhang, C., Ou, Y.B., Lin, Y., Song, B.T., Xie, C.H., Liu, J., and Li, X.Q.** (2011).
817 Systematic analysis of potato acid invertase genes reveals that a cold-responsive member,
818 *StvacINV1*, regulates cold-induced sweetening of tubers. *Mol Genet Genomics* **286**, 109-
819 118.
- 820 **Liu, X., Lin, Y., Liu, J., Song, B.T., Ou, Y.B., Zhang, H.L., Li, M., and Xie, C.H.** (2013).
821 *StInvInh2* as an inhibitor of *StvacINV1* regulates the cold-induced sweetening of potato
822 tubers by specifically capping vacuolar invertase activity. *Plant Biotechnol J* **11**, 640-647.
- 823 **Ly, D.N.P., Iqbal, S., Fosu-Nyarko, J., Milroy, S., and Jones, M.G.K.** (2023). Multiplex
824 CRISPR-Cas9 gene-editing can deliver potato cultivars with reduced browning and
825 acrylamide. *Plants* **12**, 379.
- 826 **Ma, X.L., Zhu, Q.L., Chen, Y.L., and Liu, Y.G.** (2016). CRISPR/Cas9 platforms for genome
827 editing in plants: developments and applications. *Mol Plant* **9**, 961-974.
- 828 **Ma, X.L., Zhang, Q.Y., Zhu, Q.L., Liu, W., Chen, Y., Qiu, R., Wang, B., Yang, Z.F., Li,**
829 **H.Y., Lin, Y.R., Xie, Y.Y., Shen, R.X., Chen, S.F., Wang, Z., Chen, Y.L., Guo, J.X.,**
830 **Chen, L.T., Zhao, X.C., Dong, Z.C., and Liu, Y.G.** (2015). A robust CRISPR/Cas9
831 system for convenient, high-efficiency multiplex genome editing in monocot and dicot
832 plants. *Mol Plant* **8**, 1274-1284.
- 833 **Mckenzie, M.J., Chen, R.K.Y., Harris, J.C., Ashworth, M.J., and Brummell, D.A.** (2013).
834 Post-translational regulation of acid invertase activity by vacuolar invertase inhibitor
835 affects resistance to cold-induced sweetening of potato tubers. *Plant Cell Environ* **36**,
836 176-185.
- 837 **Menendez, C.M., Ritter, E., Schafer-Pregl, R., Walkemeier, B., Kalde, A., Salamini, F., and**
838 **Gebhardt, C.** (2002). Cold sweetening in diploid potato: Mapping quantitative trait loci
839 and candidate genes. *Genetics* **162**, 1423-1434.
- 840 **Meng, F.L., Zhao, H.N., Zhu, B., Zhang, T., Yang, M.Y., Li, Y., Han, Y.P., and Jiang, J.M.**
841 (2021). Genomic editing of intronic enhancers unveils their role in fine-tuning tissue-
842 specific gene expression in *Arabidopsis thaliana*. *Plant Cell* **33**, 1997-2014.
- 843 **Mottram, D.S., Wedzicha, B.L., and Dodson, A.T.** (2002). Acrylamide is formed in the
844 Maillard reaction. *Nature* **419**, 448-449.
- 845 **Mribu, H.K., and Veilleux, R.E.** (1990). Effect of genotype, explant, subculture interval and
846 environmental conditions on regeneration of shoots from in vitro monoplasts of a diploid
847 potato species, *Solanum phureja* Juz. & Buk. *Plant Cell Tiss Org* **23**, 171-179.
- 848 **Murashige, T., and Skoog, F.** (1962). A revised medium for rapid growth and bio assays with
849 tobacco tissue cultures. *Physiol Plantarum* **15**, 473-497.

- 850 **Ou, Y.B., Song, B.T., Liu, X., Xie, C.H., Li, M., Lin, Y., Zhang, H.L., and Liu, J.** (2013).
851 Promoter regions of potato vacuolar invertase gene in response to sugars and hormones.
852 *Plant Physiol Bioch* **69**, 9-16.
- 853 **Paz, M.M., and Veilleux, R.E.** (1999). Influence of culture medium and conditions on shoot
854 regeneration in monoploids and fertility of regenerated doubled monoploids. *Plant*
855 *Breeding* **118**, 53-57.
- 856 **Pham, G.M., Hamilton, J.P., Wood, J.C., Burke, J.T., Zhao, H.N., Vaillancourt, B., Ou, S.J.,**
857 **Jiang, J.M., and Buell, C.R.** (2020). Construction of a chromosome-scale long-read
858 reference genome assembly for potato. *Gigascience* **9**, giaa100.
- 859 **Ruan, Y.L., Jin, Y., Yang, Y.J., Li, G.J., and Boyer, J.S.** (2010). Sugar input, metabolism, and
860 signaling mediated by invertase: roles in development, yield potential, and response to
861 drought and heat. *Mol Plant* **3**, 942-955.
- 862 **Sowokinos, J.R.** (2001). Biochemical and molecular control of cold-induced sweetening in
863 potatoes. *Am. J. Potato Res.* **78**, 221-236.
- 864 **Stadler, R.H., Blank, I., Varga, N., Robert, F., Hau, J., Guy, P.A., Robert, M.C., and**
865 **Riediker, S.** (2002). Acrylamide from Maillard reaction products. *Nature* **419**, 449-450.
- 866 **Tang, D., Jia, Y.X., Zhang, J.Z., Li, H.B., Cheng, L., Wang, P., Bao, Z.G., Liu, Z.H., Feng,**
867 **S.S., Zhu, X.J., Li, D.W., Zhu, G.T., Wang, H.R., Zhou, Y., Zhou, Y.F., Bryan, G.J.,**
868 **Buell, C.R., Zhang, C.Z., and Huang, S.W.** (2022). Genome evolution and diversity of
869 wild and cultivated potatoes. *Nature* **606**, 535-541.
- 870 **Tang, G.Q., Luscher, M., and Sturm, A.** (1999). Antisense repression of vacuolar and cell wall
871 invertase in transgenic carrot alters early plant development and sucrose partitioning.
872 *Plant Cell* **11**, 177-189.
- 873 **The Potato Genome Sequencing Consortium.** (2011). Genome sequence and analysis of the
874 tuber crop potato. *Nature* **475**, 189-195.
- 875 **van Os, H., Andrzejewski, S., Bakker, E., Barrena, I., Bryan, G.J., Caromel, B., Ghareeb,**
876 **B., Isidore, E., de Jong, W., van Koert, P., Lefebvre, V., Milbourne, D., Ritter, E.,**
877 **van der Voort, J.N.A.M.R., Rousselle-Bourgeois, F., van Vliet, J., Waugh, R., Visser,**
878 **R.G.F., Bakker, J., and van Eck, H.J.** (2006). Construction of a 10,000-marker
879 ultradense genetic recombination map of potato: Providing a framework for accelerated
880 gene isolation and a genomewide physical map. *Genetics* **173**, 1075-1087.
- 881 **Verma, S., and Bhatia, S.** (2019). A comprehensive analysis of the B3 superfamily identifies
882 tissue-specific and stress-responsive genes in chickpea (*Cicer arietinum* L.). *3 Biotech* **9**,
883 346.
- 884 **Wan, H.J., Wu, L.M., Yang, Y.J., Zhou, G.Z., and Ruan, Y.L.** (2018). Evolution of sucrose
885 metabolism: the dichotomy of invertases and beyond. *Trends Plant Sci* **23**, 163-177.
- 886 **Wang, L., and Ruan, Y.L.** (2016). Critical roles of vacuolar invertase in floral organ
887 development and male and female fertilities are revealed through characterization of
888 GhVIN1-RNAi cotton plants. *Plant Physiol* **171**, 405-423.
- 889 **Wang, L., Cook, A., Patrick, J.W., Chen, X.Y., and Ruan, Y.L.** (2014). Silencing the
890 vacuolar invertase gene *GhVIN1* blocks cotton fiber initiation from the ovule epidermis,
891 probably by suppressing a cohort of regulatory genes via sugar signaling. *Plant J* **78**, 686-
892 696.
- 893 **Wang, Y.P., Zhang, N., Li, T., Yang, J.W., Zhu, X., Fang, C.X., Li, S.G., and Si, H.J.** (2019).
894 Genome-wide identification and expression analysis of StTCP transcription factors of
895 potato (*Solanum tuberosum* L.). *Computational Biology and Chemistry* **78**, 53-63.

- 896 Weirauch, M.T., Yang, A., Albu, M., Cote, A.G., Montenegro-Montero, A., Drewe, P.,
897 Najafabadi, H.S., Lambert, S.A., Mann, I., Cook, K., Zheng, H., Goity, A., van
898 Bakel, H., Lozano, J.C., Galli, M., Lewsey, M.G., Huang, E.Y., Mukherjee, T., Chen,
899 X.T., Reece-Hoyes, J.S., Govindarajan, S., Shaulsky, G., Walhout, A.J.M., Bouget,
900 F.Y., Ratsch, G., Larrondo, L.F., Ecker, J.R., and Hughes, T.R. (2014).
901 Determination and inference of eukaryotic transcription factor sequence specificity. *Cell*
902 **158**, 1431-1443.
- 903 Wu, L., Bhaskar, P.B., Busse, J.S., Zhang, R.F., Bethke, P.C., and Jiang, J.M. (2011).
904 Developing cold-chipping potato varieties by silencing the vacuolar invertase gene. *Crop*
905 *Sci.* **51**, 981-990.
- 906 Xie, K.B., Minkenberg, B., and Yang, Y.N. (2015). Boosting CRISPR/Cas9 multiplex editing
907 capability with the endogenous tRNA-processing system. *Proc Natl Acad Sci USA* **112**,
908 3570-3575.
- 909 Xie, X.B., Li, S., Zhang, R.F., Zhao, J., Chen, Y.C., Zhao, Q., Yao, Y.X., You, C.X., Zhang,
910 X.S., and Hao, Y.J. (2012). The bHLH transcription factor MdbHLH3 promotes
911 anthocyanin accumulation and fruit colouration in response to low temperature in apples.
912 *Plant Cell Environ* **35**, 1884-1897.
- 913 Ye, J., Shakya, R., Shrestha, P., and Rommens, C.M. (2010). Tuber-specific silencing of the
914 acid invertase gene substantially lowers the acrylamide forming potential of potato. *J.*
915 *Agric. Food Chem.* **58**, 12162-12167.
- 916 Yu, R.M., Chang, Y.N., Chen, H.Z., Feng, J.L., Wang, H.J., Tian, T., Song, Y.J., and Gao,
917 G. (2022). Genome-wide identification of the *GATA* gene family in potato (*Solanum*
918 *tuberosum* L.) and expression analysis. *Journal of Plant Biochemistry and Biotechnology*
919 **31**, 37-48.
- 920 Yu, X.Y., Wang, X.F., Zhang, W.Q., Qian, T.T., Tang, G.M., Guo, Y.K., and Zheng, C.C.
921 (2008). Antisense suppression of an acid invertase gene (*MAII*) in muskmelon alters
922 plant growth and fruit development. *J. Exp. Bot.* **59**, 2969-2977.
- 923 Zeng, Z.X., Zhang, W.L., Marand, A.P., Zhu, B., Buell, C.R., and Jiang, J.M. (2019). Cold
924 stress induces enhanced chromatin accessibility and bivalent histone modifications
925 H3K4me3 and H3K27me3 of active genes in potato. *Genome Biol* **20**, 123.
- 926 Zhang, C., Xie, C.-H., Song, B.-T., Liu, X., and Liu, J. (2008). RNAi effects on regulation of
927 endogenous acid invertase activity in potato (*Solanum tuberosum* L.) tubers. *Chinese J.*
928 *Agri. Biotech.* **5**, 107-112.
- 929 Zhang, H., Wu, T., Li, Z., Huang, K., Kim, N.E., Ma, Z.M., Kwon, S.W., Jiang, W.Z., and
930 Du, X.L. (2021). OsGATA16, a GATA transcription factor, confers cold tolerance by
931 repressing OsWRKY45-1 at the seedling stage in rice. *Rice* **14**.
- 932 Zhang, H., Liu, S.J., Ren, T.M., Niu, M.X., Liu, X., Liu, C., Wang, H.L., Yin, W.L., and Xia,
933 X.L. (2023). Crucial abiotic stress regulatory network of NF-Y transcription factor in
934 plants. *Int J Mol Sci* **24**, 4426.
- 935 Zhang, W.L., Zhang, T., Wu, Y.F., and Jiang, J.M. (2012). Genome-wide identification of
936 regulatory DNA elements and protein-binding footprints using signatures of open
937 chromatin in *Arabidopsis*. *Plant Cell* **24**, 2719-2731.
- 938 Zhao, H.N., Zhang, W.L., Chen, L.F., Wang, L., Marand, A.P., Wu, Y.F., and Jiang, J.M.
939 (2018). Proliferation of regulatory DNA elements derived from transposable elements in
940 the maize genome. *Plant Physiol* **176**, 2789-2803.

- 941 **Zhao, H.N., Yang, M.Y., Bishop, J., Teng, Y.H., Cao, Y.X., Beall, B.D., Li, S.L., Liu, T.X.,**
942 **Fang, Q.X., Fang, C., Xin, H.Y., Nutzmann, H.W., Osbourn, A., Meng, F.L., and**
943 **Jiang, J.M.** (2022). Identification and functional validation of super-enhancers in
944 *Arabidopsis thaliana*. *Proc Natl Acad Sci U S A* **119**, e2215328119.
- 945 **Zhou, H., Zeng, R.F., Liu, T.J., Ai, X.Y., Ren, M.K., Zhou, J.J., Hu, C.G., and Zhang, J.Z.**
946 (2022). Drought and low temperature-induced NF-YA1 activates FT expression to
947 promote citrus flowering. *Plant Cell Environ* **45**, 3505-3522.
- 948 **Zhou, Q., Tang, D., Huang, W., Yang, Z.M., Zhang, Y., Hamilton, J.P., Visser, R.G.F.,**
949 **Bachem, C.W.B., Buell, C.R., Zhang, Z.H., Zhang, C.Z., and Huang, S.W.** (2020).
950 Haplotype-resolved genome analyses of a heterozygous diploid potato. *Nat Genet* **52**,
951 1018-1023.
- 952 **Zhu, B., Zhang, W.L., Zhang, T., Liu, B., and Jiang, J.M.** (2015). Genome-wide prediction
953 and validation of intergenic enhancers in *Arabidopsis* using open chromatin signatures.
954 *Plant Cell* **27**, 2415-2426.
- 955 **Zhu, X.B., Richael, C., Chamberlain, P., Busse, J.S., Bussan, A.J., Jiang, J.M., and Bethke,**
956 **P.C.** (2014). Vacuolar invertase gene silencing in potato (*Solanum tuberosum* L.)
957 improves processing quality by decreasing the frequency of sugar-end defects. *PLoS*
958 *ONE* **9**, e93381.
- 959 **Zhu, X.B., Gong, H.L., He, Q.Y., Zeng, Z.X., Busse, J.S., Jin, W.W., Bethke, P.C., and**
960 **Jiang, J.M.** (2016). Silencing of vacuolar invertase and asparagine synthetase genes and
961 its impact on acrylamide formation of fried potato products. *Plant Biotechnol J* **14**, 709-
962 718.
- 963 **Zrenner, R., Schuler, K., and Sonnewald, U.** (1996). Soluble acid invertase determines the
964 hexose-to-sucrose ratio in cold-stored potato tubers. *Planta* **198**, 246-252.

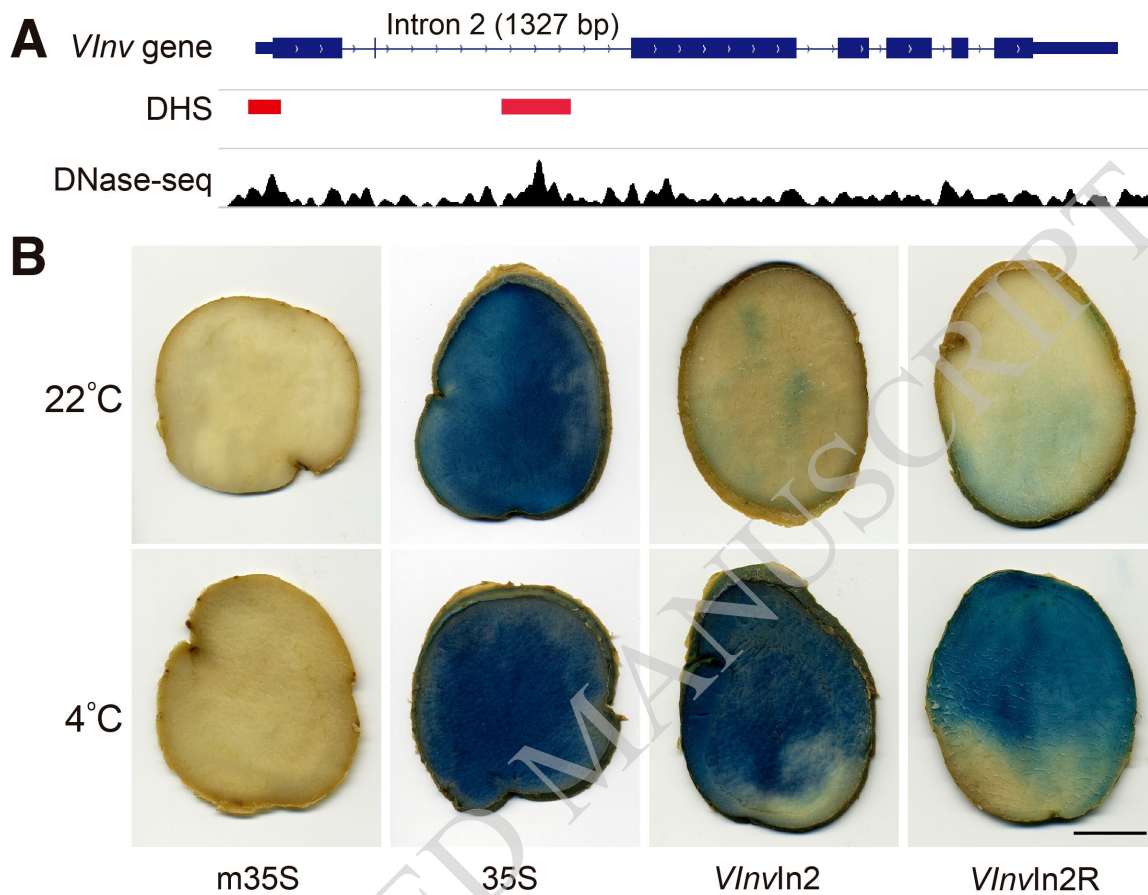


Figure 1. Discovery of a cold-responsive intronic enhancer in *Vlnv* gene.

(A) DNase-hypersensitive sites (DHSs) associated with *Vlnv* gene. DHS map was developed from tuber tissue of DM1-3 potato. Two DHSs (red bars), one at the 5' of the gene and one in the second intron, were detected.

(B) β -glucuronidase (GUS) reporter gene assays of the second intron of *Vlnv* gene in Katahdin potato. Constructs using a minimal 35S promoter (m35S) and a full-length 35S promoters were used as negative and positive controls. Tubers from transgenic Katahdin lines developed using the intronic construct (*VlnvIn2*) and a reverse construct (*VlnvIn2R*) showed minimal GUS signals under room temperature (22°C). Strong GUS signals were detected from tubers after 4 weeks of cold storage under 4°C. The scale bar represents 2 cm.

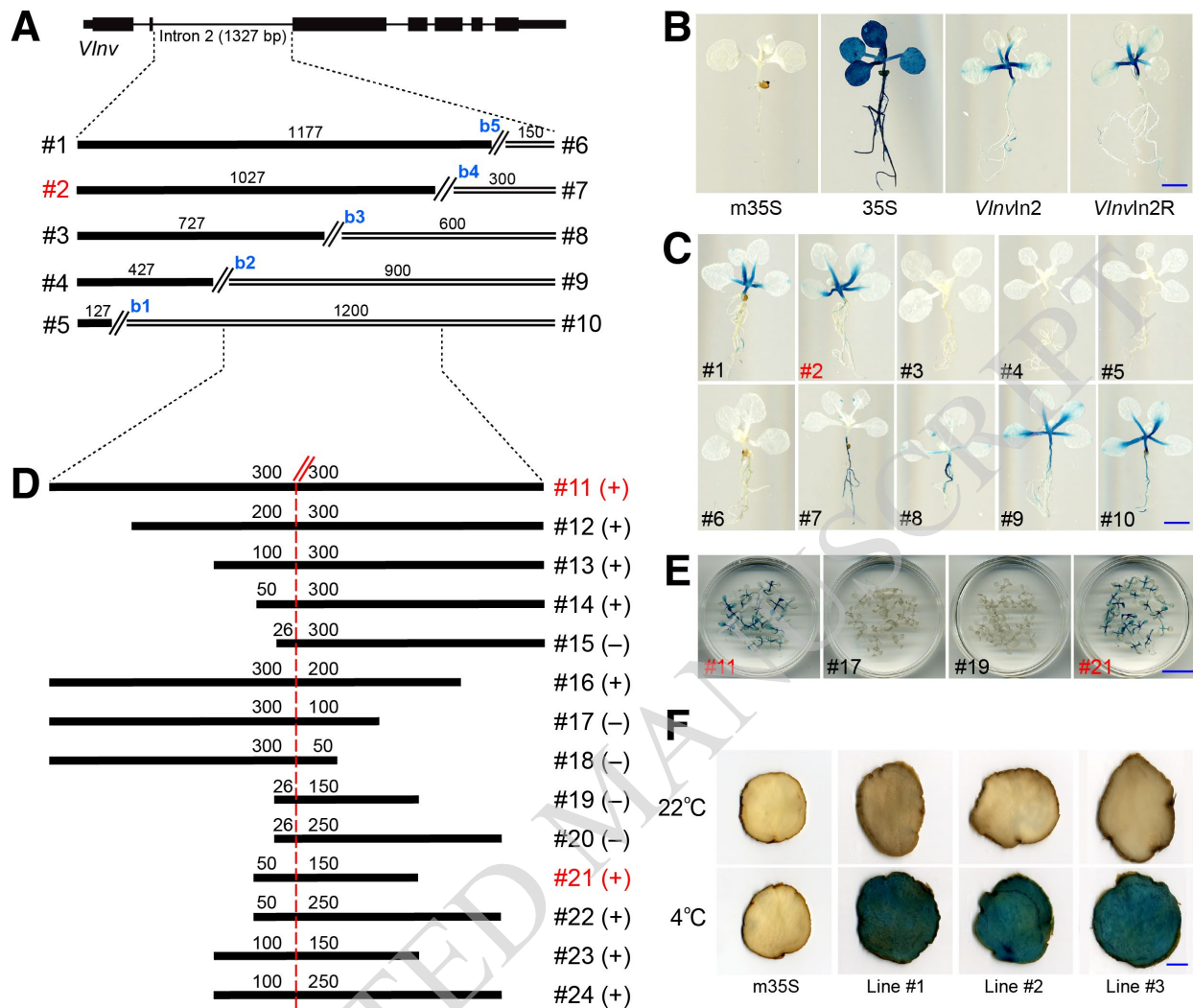


Figure 2. Identification of transcriptional enhancers in intron 2 of *Vlnv* gene.

(A) A diagram illustrating the sizes and positions of 10 sub-fragments derived from intron 2 of the *Vlnv* gene. The 1327-bp intron was divided into ten fragments (#1 to #10) using five breaks (b1 to b5).

(B) β -glucuronidase (GUS) reporter gene assays of the intron 2 in *A. thaliana*. Constructs with minimal 35S promoter (m35S) and a full-length 35S promoter (35S) were used as negative and positive controls.

(C) GUS expression patterns of representative *A. thaliana* transgenic seedlings derived from each of the ten constructs consisting of a fragment ligated with the m35S promoter and the GUS reporter gene.

(D) A diagram illustrating the sizes and positions of the 13 fragments derived from the DNA fragment #11. A dashed red line marks the middle point of the 600-bp segment #11. "+" and "-" indicate the derived transgenic seedlings showing positive and negative GUS signals, respectively.

(E) GUS staining of 20 *A. thaliana* transgenic seedlings derived from constructs #11, #17, #19, and #21, respectively.

(F) GUS reporter gene assay of the 200-bp *VlnvIn2En* enhancer in Katahdin potato. Tubers from three independent transgenic lines showed minimal GUS signals under 22°C but strong signals from tubers after 4 weeks of cold storage under 4°C.

All numbers above bars/lines in (A) and (D) indicate base pairs. The scale bar represents 2 mm in (B, C) and 1 cm in (E, F). Fragment numbers highlighted in red color in (A, C, D, E) indicate representative constructs with full enhancer function.

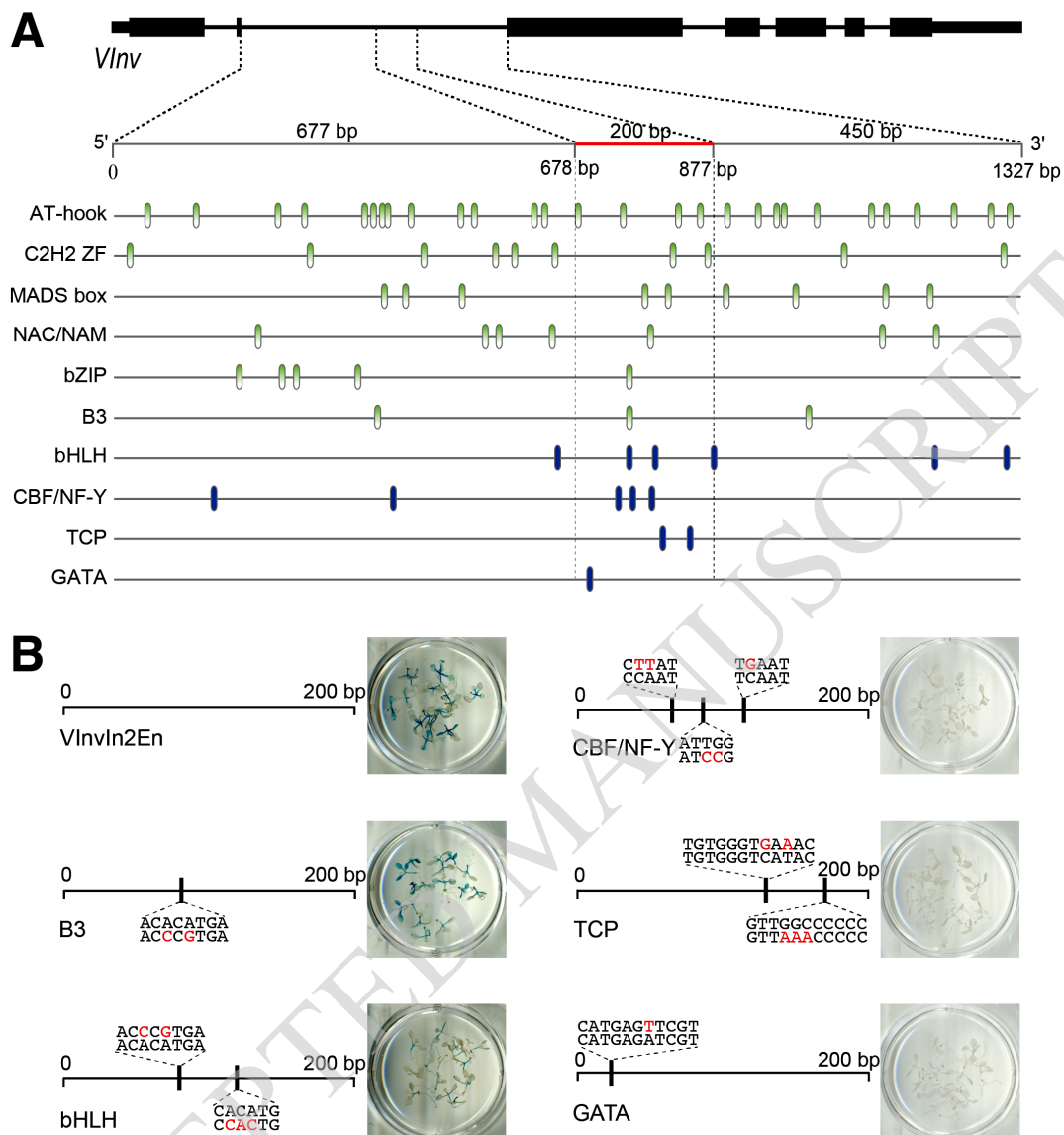


Figure 3. Distribution and function of DNA motifs in intron 2 and the *VlnvIn2En* enhancer.

(A) Distribution of DNA motifs related to transcription factors (TFs) involved in response to cold stress. Each vertical bar represents a potential TF-binding site. A red horizontal bar marks the position of the 200-bp enhancer. Vertical blue bars indicate that the binding sites of a relevant TF are enriched or exclusively located within the 200-bp enhancer. Vertical green bars indicate that the binding sites of a relevant TF are not enriched within the enhancer

(B) Transgenic assays of *VlnvIn2En* with mutated DNA motifs related to five different TFs. Red colored nucleotides indicate the replaced sequence(s) in each construct. No β -glucuronidase (GUS) signals were detected in any transgenic *A. thaliana* plants derived from the three constructs with mutated motifs related to CBF/NF-Y, TCP, and GATA.

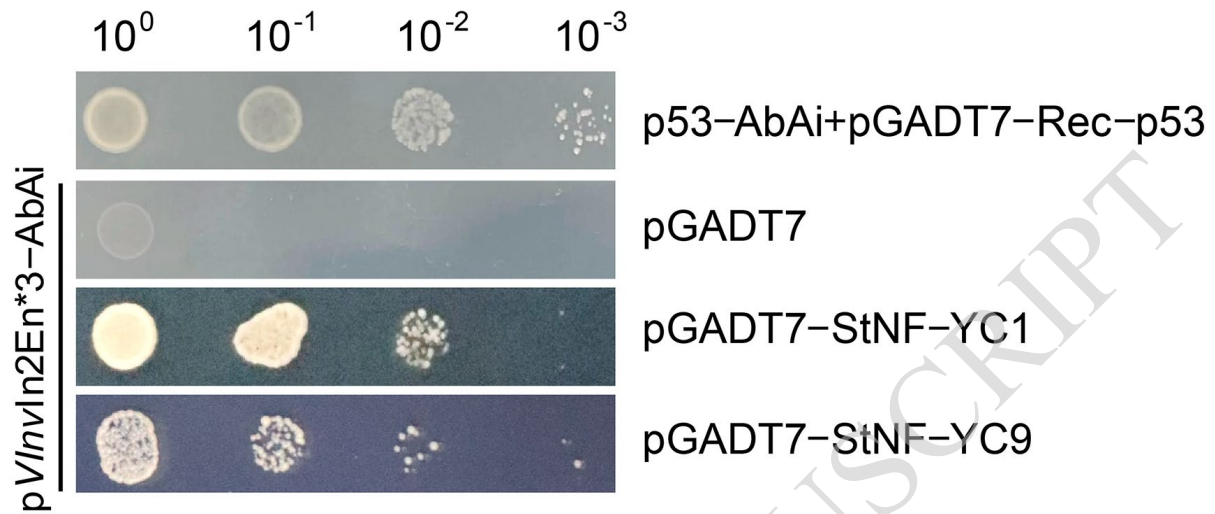


Figure 4. Identification of StNF-YC1 and StNF-YC9 proteins that bind to *VlnVln2En* using yeast one-hybrid assay. Triple copies of the *VlnVln2En* sequence (*VlnVln2En*3*) were synthesized to develop the bait plasmid $pVlnVln2En^*3-AbAi$. The pGADT7 vector was used as negative control, and a combination of two constructs ($p53-AbAi$ and $pGADT7-Rec-p53$) was used as positive control.

ACCEPTED MANUSCRIPT

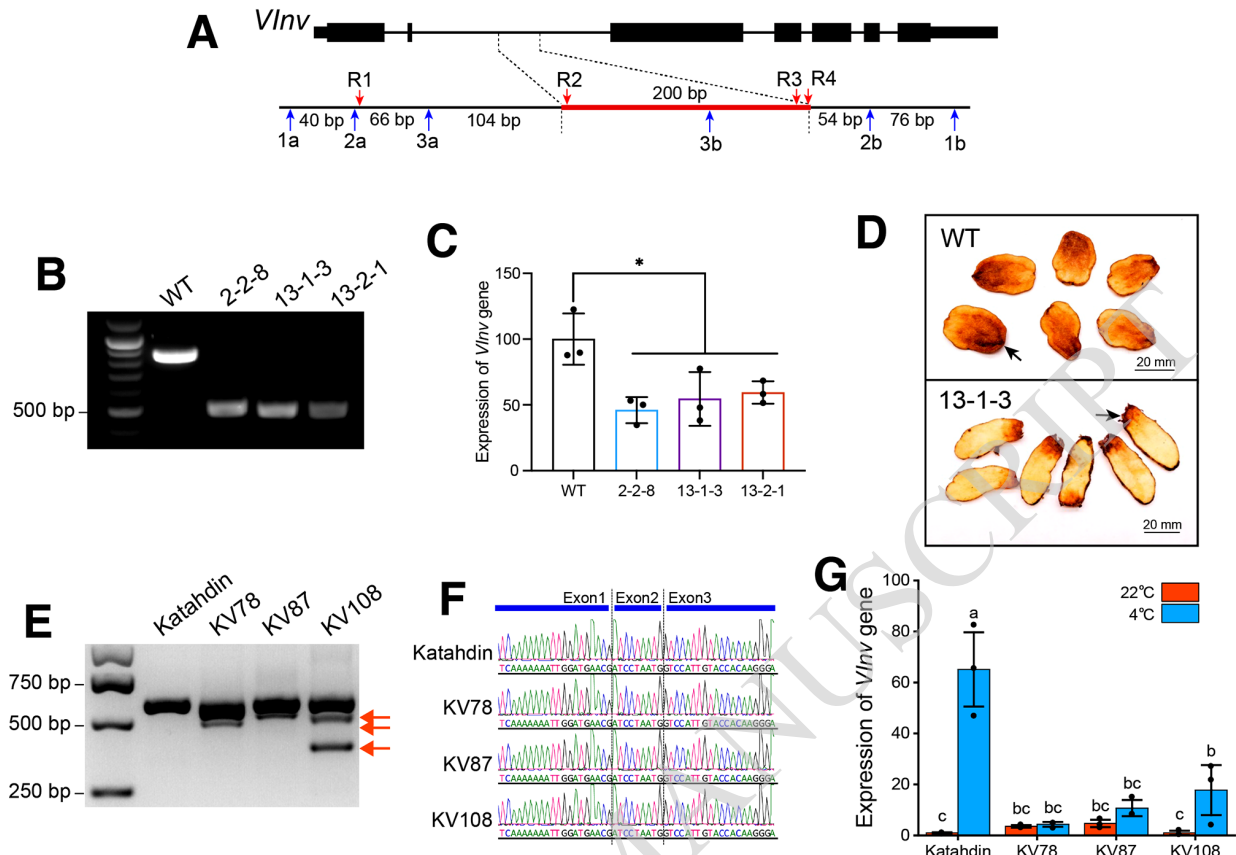


Figure 5. Functional validation of the *VlnvIn2En* enhancer using genome editing.

(A) A diagram illustrating the positions of all sgRNAs within and outside of intron 2 of *Vlnv* gene. The red bar marks the 200-bp enhancer *VlnvIn2En*. Red arrows indicate the position of sgRNAs R1, R2, R3, and R4. Blue arrows indicate the position of sgRNAs 1a, 2a, 3a, 1b, 2b, and 3b.

(B) Gel electrophoresis of PCR products amplified from the three homozygous CRISPR/Cas9 deletion lines (2-2-8, 13-1-3 and 13-2-1) developed from the wild-type (WT) DMF5-73-1.

(C) Reverse transcription quantitative PCR (RT-qPCR)-based transcription analysis of *Vlnv* gene in cold-stored potato tissues from the three homozygous deletion lines (2-2-8, 13-1-3 and 13-2-1). All three lines showed significant reduction of *Vlnv* expression relative to the *Actin97* reference gene. The y axis represents the relative expression level normalized by setting *Vlnv* expression in cold-stored tubers of the wild-type (WT) DMF5-73-1 to 1. Data is presented as mean \pm standard deviation (SD) from three biological replicates and was tested by the Student *t*-test ($*P < 0.05$).

(D) Chipping of tubers from deletion line 13-1-3 and from the WT DMF5-73-1. Note: (1) the dark color toward one end of each chip is caused by the “jelly end” problem (two examples are indicated by arrows) associated with both 13-1-3 and WT. (2) 13-1-3 is a selfed progeny of a T0 DMF5-73-1 (heterozygous) transgenic line. Thus, the tubers from the two lines show different shapes. Three tubers from each line were used for chipping, and two chips from each tuber were included in the illustration.

(E) Gel electrophoresis of PCR products amplified from the genomic DNA of three T0 CRISPR/Cas9 lines (KV78, KV87 and KV108) developed from tetraploid potato cultivar Katahdin. Red arrows indicate fragments resulted from deletions within *VlnvIn2En*.

(F) Sequencing of PCR products amplified from cDNAs of the three CRISPR/Cas9 lines. Normal splicing between exon 1 and exon 3 was detected in all three lines.

(G) Reverse transcription quantitative (RT-qPCR)-based analysis of *Vlnv* expression relative to the *Actin97* gene of the three CRISPR/Cas lines. Expression was analyzed using tubers after 2 weeks of storage at 22°C and 4°C, respectively. The y axis represents the relative expression level normalized by setting *Vlnv* expression in 22°C-stored tubers of the wild-type Katahdin to 1. Data is presented as mean \pm standard deviation (SD) from three biological replicates and were tested by using PROC GLM analyses of variance (ANOVA). Different lower case letters represent statistically significant differences at $P = 0.05$.

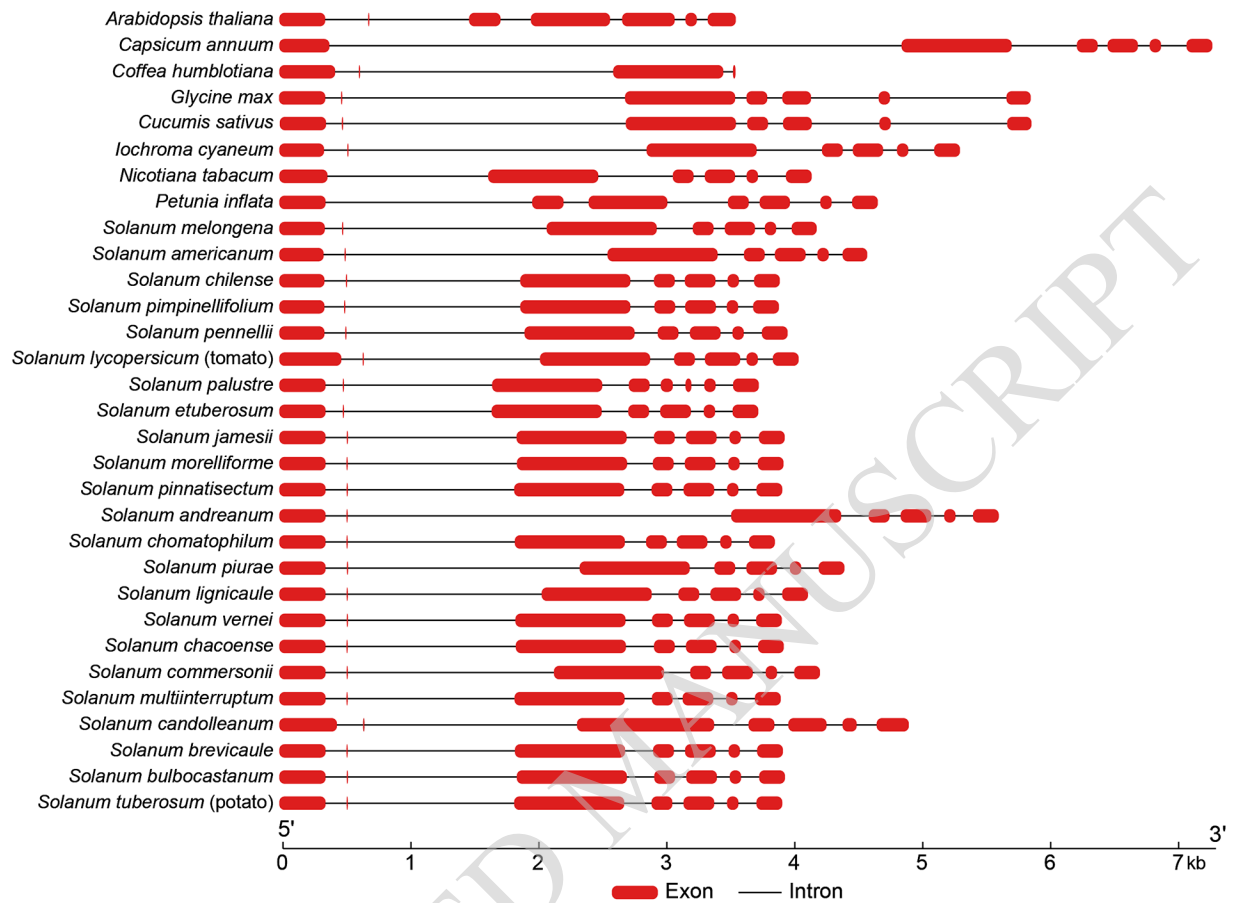


Figure 6. Composition of introns and exons of *Vlnv* genes from different plant species. A total of 28 Solanaceous species and eight distantly related dicot species were selected for the analysis. The distinctly small exon 2 (9 bp) was detected in all Solanaceous species, as well as in five distantly related plant species. In addition, a large intron 2 (ranging from 780 bp to 2,997 bp) following the small exon 2, was identified in most plant species.

Parsed Citations

- Agarwal, S., Chakrabarti, S.K., Shikha, M., Chimote, V.P., Pattanayak, D., and Naik, P.S. (2003). A biotechnological approach for reduction of cold-induced sweetening in potato tubers. *J. Indian Potato Assoc.* 30, 39-40.
Google Scholar: [Author Only](#) [Title Only](#) [Author and Title](#)
- Amrein, T.M., Bachmann, S., Noti, A., Biedermann, M., Barbosa, M.F., Biedermann-Brem, S., Grob, K., Keiser, A., Realini, P., Escher, F., and Arnado, R. (2003). Potential of acrylamide formation, sugars, and free asparagine in potatoes: A comparison of cultivars and farming systems. *J. Agric. Food Chem.* 51, 5556-5560.
Google Scholar: [Author Only](#) [Title Only](#) [Author and Title](#)
- Bagnaresi, P., Moschella, A., Beretta, O., Vitulli, F., Ranalli, P., and Perata, P. (2008). Heterologous microarray experiments allow the identification of the early events associated with potato tuber cold sweetening. *BMC Genomics* 9, 176.
Google Scholar: [Author Only](#) [Title Only](#) [Author and Title](#)
- Becalski, A., Lau, B.P.Y., Lewis, D., Seaman, S.W., Hayward, S., Sahagian, M., Ramesh, M., and Leclerc, Y. (2004). Acrylamide in french fries: Influence of free amino acids and sugars. *J. Agric. Food Chem.* 52, 3801-3806.
Google Scholar: [Author Only](#) [Title Only](#) [Author and Title](#)
- Bhaskar, P.B., Raasch, J.A., Kramer, L.C., Neumann, P., Wielgus, S.M., Austin-Phillips, S., and Jiang, J.M. (2008). Sgt1, but not Rar1, is essential for the RB-mediated broad-spectrum resistance to potato late blight. *BMC Plant Biol.* 8, 8.
Google Scholar: [Author Only](#) [Title Only](#) [Author and Title](#)
- Bhaskar, P.B., Wu, L., Busse, J.S., Whitty, B.R., Hamernik, A.J., Jansky, S.H., Buell, C.R., Bethke, P.C., and Jiang, J.M. (2010). Suppression of the vacuolar invertase gene prevents cold-induced sweetening in potato. *Plant Physiol.* 154, 939-948.
Google Scholar: [Author Only](#) [Title Only](#) [Author and Title](#)
- Braun, S.R., Endelman, J.B., Haynes, K.G., and Jansky, S.H. (2017). Quantitative trait loci for resistance to common scab and cold-induced sweetening in diploid potato. *Plant Genome* 10, DOI: 10.3835/plantgenome2016.3810.0110.
Google Scholar: [Author Only](#) [Title Only](#) [Author and Title](#)
- Brummell, D.A., Chen, R.K.Y., Harris, J.C., Zhang, H.B., Hamiaux, C., Kralicek, A.V., and McKenzie, M.J. (2011). Induction of vacuolar invertase inhibitor mRNA in potato tubers contributes to cold-induced sweetening resistance and includes spliced hybrid mRNA variants. *J Exp Bot* 62, 3519-3534.
Google Scholar: [Author Only](#) [Title Only](#) [Author and Title](#)
- Butler, N.M., Jansky, S.H., and Jiang, J.M. (2020). First-generation genome editing in potato using hairy root transformation. *Plant Biotechnol J* 18, 2201-2209.
Google Scholar: [Author Only](#) [Title Only](#) [Author and Title](#)
- Byrne, S., Meade, F., Mesiti, F., Griffin, D., Kennedy, C., and Milbourne, D. (2020). Genome-wide association and genomic prediction for fry color in potato. *Agronomy-Basel* 10, 90.
Google Scholar: [Author Only](#) [Title Only](#) [Author and Title](#)
- Cermak, T., Curtin, S.J., Gil-Humanes, J., Cegan, R., Kono, T.J.Y., Konecna, E., Belanto, J.J., Starker, C.G., Mathre, J.W., Greenstein, R.L., and Voytasa, D.F. (2017). A multipurpose toolkit to enable advanced genome engineering in plants. *Plant Cell* 29, 1196-1217.
Google Scholar: [Author Only](#) [Title Only](#) [Author and Title](#)
- Chen, C.J., Chen, H., Zhang, Y., Thomas, H.R., Frank, M.H., He, Y.H., and Xia, R. (2020). TBtools: an integrative toolkit developed for interactive analyses of big biological data. *Mol Plant* 13, 1194-1202.
Google Scholar: [Author Only](#) [Title Only](#) [Author and Title](#)
- Chen, R.G., Ma, J.H., Luo, D., Hou, X.M., Ma, F., Zhang, Y.M., Meng, Y.C., Zhang, H.F., and Guo, W.L. (2019). CaMADS, a MADS-box transcription factor from pepper, plays an important role in the response to cold, salt, and osmotic stress. *Plant Sci* 280, 164-174.
Google Scholar: [Author Only](#) [Title Only](#) [Author and Title](#)
- Chow, C.N., Lee, T.Y., Hung, Y.C., Li, G.Z., Tseng, K.C., Liu, Y.H., Kuo, P.L., Zheng, H.Q., and Chang, W.C. (2019). PlantPAN3.0: a new and updated resource for reconstructing transcriptional regulatory networks from ChIP-seq experiments in plants. *Nucleic Acids Res* 47, D1155-D1163.
Google Scholar: [Author Only](#) [Title Only](#) [Author and Title](#)
- Clasen, B.M., Stoddard, T.J., Luo, S., Demorest, Z.L., Li, J., Cedrone, F., Tibebu, R., Davison, S., Ray, E.E., Daulhac, A., Coffman, A., Yabandith, A., Retterath, A., Haun, W., Baltus, N.J., Mathis, L., Voytas, D.F., and Zhang, F. (2016). Improving cold storage and processing traits in potato through targeted gene knockout. *Plant Biotechnol J* 14, 169-176.
Google Scholar: [Author Only](#) [Title Only](#) [Author and Title](#)
- Clough, S.J., and Bent, A.F. (1998). Floral dip: a simplified method for *Agrobacterium*-mediated transformation of *Arabidopsis thaliana*. *Plant J.* 16, 735-743.
Google Scholar: [Author Only](#) [Title Only](#) [Author and Title](#)

Dahro, B., Wang, Y., Khan, M., Zhang, Y., Fang, T., Ming, R.H., Li, C.L., and Liu, J.H. (2022). Two AT-Hook proteins regulate A/NIN7 expression to modulate sucrose catabolism for cold tolerance in *Poncirus trifoliata*. *New Phytol* 235, 2331-2349.

Google Scholar: [Author Only](#) [Title Only](#) [Author and Title](#)

Dale, M.F.B., and Bradshaw, J.E. (2003). Progress in improving processing attributes in potato. *Trends Plant Sci* 8, 310-312.

Google Scholar: [Author Only](#) [Title Only](#) [Author and Title](#)

Deng, X.S., Han, X.H., Yu, S.C., Liu, Z.J., Guo, D.M., He, Y., Li, W.Y., Tao, Y., Sun, C.W., Xu, P.Z., Liao, Y.X., Chen, X.Q., Zhang, H.Y., and Wu, X.J. (2020). OsINV3 and its homolog, OsINV2, control grain size in rice. *Int J Mol Sci* 21, 2199.

Google Scholar: [Author Only](#) [Title Only](#) [Author and Title](#)

Devaux, A., Goffart, J.-P., Petsakos, A., Kromann, P., Gatto, M., Okello, J., Suarez, V., and Hareau, G. (2020). Global food security, contributions from sustainable potato agri-food systems. In *The potato crop: its agricultural, nutritional and social contribution to humankind*, H. Campos, Ortiz, O., ed (Dordrecht: Springer), pp. 3-35.

Google Scholar: [Author Only](#) [Title Only](#) [Author and Title](#)

Draffehn, A.M., Meller, S., Li, L., and Gebhardt, C. (2010). Natural diversity of potato (*Solanum tuberosum*) invertases. *BMC Plant Biology* 10, 271.

Google Scholar: [Author Only](#) [Title Only](#) [Author and Title](#)

Endelman, J.B., and Jansky, S.H. (2016). Genetic mapping with an inbred line-derived F2 population in potato. *Theor Appl Genet* 129, 935-943.

Google Scholar: [Author Only](#) [Title Only](#) [Author and Title](#)

Fang, C., Yang, M.Y., Tang, Y.C., Zhang, L., Zhao, H.N., Ni, H.J., Chen, Q.S., Meng, F.L., and Jiang, J.M. (2023). Dynamics of cis-regulatory sequences and transcriptional divergence of duplicated genes in soybean. *Proc Natl Acad Sci U S A* 120, e2303836120.

Google Scholar: [Author Only](#) [Title Only](#) [Author and Title](#)

Fischer, M., Schreiber, L., Colby, T., Kuckenberger, M., Tacke, E., Hofferbert, H.R., Schmidt, J., and Gebhardt, C. (2013). Novel candidate genes influencing natural variation in potato tuber cold sweetening identified by comparative proteomics and association mapping. *Bmc Plant Biology* 13, 113.

Google Scholar: [Author Only](#) [Title Only](#) [Author and Title](#)

Greiner, S., Rausch, T., Sonnewald, U., and Herbers, K. (1999). Ectopic expression of a tobacco invertase inhibitor homolog prevents cold-induced sweetening of potato tubers. *Nat. Biotech.* 17, 708-711.

Google Scholar: [Author Only](#) [Title Only](#) [Author and Title](#)

He, F., Li, H.G., Wang, J.J., Su, Y.Y., Wang, H.L., Feng, C.H., Yang, Y.L., Niu, M.X., Liu, C., Yin, W.L., and Xia, X.L. (2019). PeSTZ1, a C2H2-type zinc finger transcription factor from *Populus euphratica*, enhances freezing tolerance through modulation of ROS scavenging by directly regulating PeAPX2. *Plant Biotechnol J* 17, 2169-2183.

Google Scholar: [Author Only](#) [Title Only](#) [Author and Title](#)

Hu, B., Jin, J.P., Guo, A.Y., Zhang, H., Luo, J.C., and Gao, G. (2015). GSDS 2.0: an upgraded gene feature visualization server. *Bioinformatics* 31, 1296-1297.

Google Scholar: [Author Only](#) [Title Only](#) [Author and Title](#)

Hu, N., Xian, Z.Q., Li, N., Liu, Y.D., Huang, W., Yan, F., Su, D.D., Chen, J.X., and Li, Z.G. (2019). Rapid and user-friendly open-source CRISPR/Cas9 system for single- or multi-site editing of tomato genome. *Hortic Res-England* 6, 7.

Google Scholar: [Author Only](#) [Title Only](#) [Author and Title](#)

Jansky, S.H., Chung, Y.S., and Kittipadukul, P. (2014). M6: A diploid potato inbred line for use in breeding and genetics research. *Journal of Plant Registrations* 8, 195-199.

Google Scholar: [Author Only](#) [Title Only](#) [Author and Title](#)

Jiang, J.M. (2015). The 'dark matter' in the plant genomes: non-coding and unannotated DNA sequences associated with open chromatin. *Curr Opin Plant Biol* 24, 17-23.

Google Scholar: [Author Only](#) [Title Only](#) [Author and Title](#)

Klann, E.M., Hall, B., and Bennett, A.B. (1996). Antisense acid invertase (TIV1) gene alters soluble sugar composition and size in transgenic tomato fruit. *Plant Physiol.* 112, 1321-1330.

Google Scholar: [Author Only](#) [Title Only](#) [Author and Title](#)

Kumar, S., Stecher, G., Li, M., Knyaz, C., and Tamura, K. (2018). MEGA X: molecular evolutionary genetics analysis across computing platforms. *Molecular Biology and Evolution* 35, 1547-1549.

Google Scholar: [Author Only](#) [Title Only](#) [Author and Title](#)

Kumar, S., Suleski, M., Craig, J.M., Kasparowicz, A.E., Sanderford, M., Li, M., Stecher, G., and Hedges, S.B. (2022). TimeTree 5: an expanded resource for species divergence times. *Molecular Biology and Evolution* 39, msac174.

Google Scholar: [Author Only](#) [Title Only](#) [Author and Title](#)

Lee, D.W., Lee, S.K., Rahman, M.M., Kim, Y.J., Zhang, D.B., and Jeon, J.S. (2019). The role of rice vacuolar invertase2 in seed size control. *Molecules and Cells* 42, 711-720.

Google Scholar: [Author Only](#) [Title Only](#) [Author and Title](#)

Li, L., Paulo, M.J., Strahwald, J., Lubeck, J., Hofferbert, H.R., Tacke, E., Junghans, H., Wunder, J., Draffehn, A., van Eeuwijk, F., and Gebhardt, C. (2008). Natural DNA variation at candidate loci is associated with potato chip color, tuber starch content, yield and starch yield. *Theor. Appl. Genet.* 116, 1167-1181.

Google Scholar: [Author Only](#) [Title Only](#) [Author and Title](#)

Li, S.G., Zhang, N., Zhu, X., Ma, R., Liu, S.Y., Wang, X., Yang, J.W., and Si, H.J. (2021). Genome-wide analysis of NF-Y genes in potato and functional identification of StNF-YC9 in drought tolerance. *Front Plant Sci* 12, 749688

Google Scholar: [Author Only](#) [Title Only](#) [Author and Title](#)

Li, X., Yang, Q., Liao, X.Q., Tian, Y.C., Zhang, F., Zhang, L., and Liu, Q.L. (2022a). A natural antisense RNA improves chrysanthemum cold tolerance by regulating the transcription factor DgTCP1. *Plant Physiol* 190, 605-620.

Google Scholar: [Author Only](#) [Title Only](#) [Author and Title](#)

Li, X.D., Zhuang, K.Y., Liu, Z.M., Yang, D.Y., Ma, N.N., and Meng, Q.W. (2016). Overexpression of a novel NAC-type tomato transcription factor, SINAM1, enhances the chilling stress tolerance of transgenic tobacco. *J Plant Physiol* 204, 54-65.

Google Scholar: [Author Only](#) [Title Only](#) [Author and Title](#)

Li, Z.Y., Fu, D.Y., Wang, X., Zeng, R., Zhang, X., Tian, J.G., Zhang, S.S., Yang, X.H., Tian, F., Lai, J.S., Shi, Y.T., and Yang, S.H. (2022b). The transcription factor bZIP68 negatively regulates cold tolerance in maize. *Plant Cell* 34, 2833-2851.

Google Scholar: [Author Only](#) [Title Only](#) [Author and Title](#)

Liu, C.T., Ou, S.J., Mao, B.G., Tang, J.Y., Wang, W., Wang, H.R., Cao, S.Y., Schlappi, M.R., Zhao, B.R., Xiao, G.Y., Wang, X.P., and Chu, C.C. (2018). Early selection of bZIP73 facilitated adaptation of japonica rice to cold climates. *Nat Commun* 9, 3302.

Google Scholar: [Author Only](#) [Title Only](#) [Author and Title](#)

Liu, H., Ding, Y.D., Zhou, Y.Q., Jin, W.Q., Xie, K.B., and Chen, L.L. (2017). CRISPR-P 2.0: an improved CRISPR-Cas9 tool for genome editing in plants. *Mol Plant* 10, 530-532.

Google Scholar: [Author Only](#) [Title Only](#) [Author and Title](#)

Liu, X., Song, B.T., Zhang, H.L., Li, X.Q., Xie, C.H., and Liu, J. (2010). Cloning and molecular characterization of putative invertase inhibitor genes and their possible contributions to cold-induced sweetening of potato tubers. *Mol Genet Genomics* 284, 147-159.

Google Scholar: [Author Only](#) [Title Only](#) [Author and Title](#)

Liu, X., Zhang, C., Ou, Y.B., Lin, Y., Song, B.T., Xie, C.H., Liu, J., and Li, X.Q. (2011). Systematic analysis of potato acid invertase genes reveals that a cold-responsive member, StvacINV1, regulates cold-induced sweetening of tubers. *Mol Genet Genomics* 286, 109-118.

Google Scholar: [Author Only](#) [Title Only](#) [Author and Title](#)

Liu, X., Lin, Y., Liu, J., Song, B.T., Ou, Y.B., Zhang, H.L., Li, M., and Xie, C.H. (2013). StInvInh2 as an inhibitor of StvacINV1 regulates the cold-induced sweetening of potato tubers by specifically capping vacuolar invertase activity. *Plant Biotechnol J* 11, 640-647.

Google Scholar: [Author Only](#) [Title Only](#) [Author and Title](#)

Ly, D.N.P., Iqbal, S., Fosu-Nyarko, J., Milroy, S., and Jones, M.G.K. (2023). Multiplex CRISPR-Cas9 gene-editing can deliver potato cultivars with reduced browning and acrylamide. *Plants* 12, 379.

Google Scholar: [Author Only](#) [Title Only](#) [Author and Title](#)

Ma, X.L., Zhu, Q.L., Chen, Y.L., and Liu, Y.G. (2016). CRISPR/Cas9 platforms for genome editing in plants: developments and applications. *Mol Plant* 9, 961-974.

Google Scholar: [Author Only](#) [Title Only](#) [Author and Title](#)

Ma, X.L., Zhang, Q.Y., Zhu, Q.L., Liu, W., Chen, Y., Qiu, R., Wang, B., Yang, Z.F., Li, H.Y., Lin, Y.R., Xie, Y.Y., Shen, R.X., Chen, S.F., Wang, Z., Chen, Y.L., Guo, J.X., Chen, L.T., Zhao, X.C., Dong, Z.C., and Liu, Y.G. (2015). A robust CRISPR/Cas9 system for convenient, high-efficiency multiplex genome editing in monocot and dicot plants. *Mol Plant* 8, 1274-1284.

Google Scholar: [Author Only](#) [Title Only](#) [Author and Title](#)

Mckenzie, M.J., Chen, R.K.Y., Harris, J.C., Ashworth, M.J., and Brummell, D.A. (2013). Post-translational regulation of acid invertase activity by vacuolar invertase inhibitor affects resistance to cold-induced sweetening of potato tubers. *Plant Cell Environ* 36, 176-185.

Google Scholar: [Author Only](#) [Title Only](#) [Author and Title](#)

Menendez, C.M., Ritter, E., Schafer-Pregl, R., Walkemeier, B., Kalde, A., Salamini, F., and Gebhardt, C. (2002). Cold sweetening in diploid potato: Mapping quantitative trait loci and candidate genes. *Genetics* 162, 1423-1434.

Google Scholar: [Author Only](#) [Title Only](#) [Author and Title](#)

Meng, F.L., Zhao, H.N., Zhu, B., Zhang, T., Yang, M.Y., Li, Y., Han, Y.P., and Jiang, J.M. (2021). Genomic editing of intronic

enhancers unveils their role in fine-tuning tissue-specific gene expression in *Arabidopsis thaliana*. *Plant Cell* 33, 1997-2014.

Google Scholar: [Author Only](#) [Title Only](#) [Author and Title](#)

Mottram, D.S., Wedzicha, B.L., and Dodson, A.T. (2002). Acrylamide is formed in the Maillard reaction. *Nature* 419, 448-449.

Google Scholar: [Author Only](#) [Title Only](#) [Author and Title](#)

Mribu, H.K., and Veilleux, R.E. (1990). Effect of genotype, explant, subculture interval and environmental conditions on regeneration of shoots from in vitro monoplasts of a diploid potato species, *Solanum phureja* Juz. & Buk. *Plant Cell Tiss Org* 23, 171-179.

Google Scholar: [Author Only](#) [Title Only](#) [Author and Title](#)

Murashige, T., and Skoog, F. (1962). A revised medium for rapid growth and bio assays with tobacco tissue cultures. *Physiol Plantarum* 15, 473-497.

Google Scholar: [Author Only](#) [Title Only](#) [Author and Title](#)

Ou, Y.B., Song, B.T., Liu, X., Xie, C.H., Li, M., Lin, Y., Zhang, H.L., and Liu, J. (2013). Promoter regions of potato vacuolar invertase gene in response to sugars and hormones. *Plant Physiol Bioch* 69, 9-16.

Google Scholar: [Author Only](#) [Title Only](#) [Author and Title](#)

Paz, M.M., and Veilleux, R.E. (1999). Influence of culture medium and conditions on shoot regeneration in monoplasts and fertility of regenerated doubled monoplasts. *Plant Breeding* 118, 53-57.

Google Scholar: [Author Only](#) [Title Only](#) [Author and Title](#)

Pham, G.M., Hamilton, J.P., Wood, J.C., Burke, J.T., Zhao, H.N., Vaillancourt, B., Ou, S.J., Jiang, J.M., and Buell, C.R. (2020). Construction of a chromosome-scale long-read reference genome assembly for potato. *Gigascience* 9, gaaa100.

Google Scholar: [Author Only](#) [Title Only](#) [Author and Title](#)

Ruan, Y.L., Jin, Y., Yang, Y.J., Li, G.J., and Boyer, J.S. (2010). Sugar input, metabolism, and signaling mediated by invertase: roles in development, yield potential, and response to drought and heat. *Mol Plant* 3, 942-955.

Google Scholar: [Author Only](#) [Title Only](#) [Author and Title](#)

Sowokinos, J.R. (2001). Biochemical and molecular control of cold-induced sweetening in potatoes. *Am. J. Potato Res.* 78, 221-236.

Google Scholar: [Author Only](#) [Title Only](#) [Author and Title](#)

Stadler, R.H., Blank, I., Varga, N., Robert, F., Hau, J., Guy, P.A., Robert, M.C., and Riediker, S. (2002). Acrylamide from Maillard reaction products. *Nature* 419, 449-450.

Google Scholar: [Author Only](#) [Title Only](#) [Author and Title](#)

Tang, D., Jia, Y.X., Zhang, J.Z., Li, H.B., Cheng, L., Wang, P., Bao, Z.G., Liu, Z.H., Feng, S.S., Zhu, X.J., Li, D.W., Zhu, G.T., Wang, H.R., Zhou, Y., Zhou, Y.F., Bryan, G.J., Buell, C.R., Zhang, C.Z., and Huang, S.W. (2022). Genome evolution and diversity of wild and cultivated potatoes. *Nature* 606, 535-541.

Google Scholar: [Author Only](#) [Title Only](#) [Author and Title](#)

Tang, G.Q., Luscher, M., and Sturm, A. (1999). Antisense repression of vacuolar and cell wall invertase in transgenic carrot alters early plant development and sucrose partitioning. *Plant Cell* 11, 177-189.

Google Scholar: [Author Only](#) [Title Only](#) [Author and Title](#)

The Potato Genome Sequencing Consortium. (2011). Genome sequence and analysis of the tuber crop potato. *Nature* 475, 189-195.

Google Scholar: [Author Only](#) [Title Only](#) [Author and Title](#)

van Os, H., Andrzejewski, S., Bakker, E., Barrena, I., Bryan, G.J., Caromel, B., Ghareeb, B., Isidore, E., de Jong, W., van Koert, P., Lefebvre, V., Milbourne, D., Ritter, E., van der Voort, J.N.A.M.R., Roussele-Bourgeois, F., van Mliet, J., Waugh, R., Visser, R.G.F., Bakker, J., and van Eck, H.J. (2006). Construction of a 10,000-marker ultradense genetic recombination map of potato: Providing a framework for accelerated gene isolation and a genomewide physical map. *Genetics* 173, 1075-1087.

Google Scholar: [Author Only](#) [Title Only](#) [Author and Title](#)

Verma, S., and Bhatia, S. (2019). A comprehensive analysis of the B3 superfamily identifies tissue-specific and stress-responsive genes in chickpea (*Cicer arietinum* L.). *3 Biotech* 9, 346.

Google Scholar: [Author Only](#) [Title Only](#) [Author and Title](#)

Wan, H.J., Wu, L.M., Yang, Y.J., Zhou, G.Z., and Ruan, Y.L. (2018). Evolution of sucrose metabolism: the dichotomy of invertases and beyond. *Trends Plant Sci* 23, 163-177.

Google Scholar: [Author Only](#) [Title Only](#) [Author and Title](#)

Wang, L., and Ruan, Y.L. (2016). Critical roles of vacuolar invertase in floral organ development and male and female fertilities are revealed through characterization of GhVIN1-RNAi cotton plants. *Plant Physiol* 171, 405-423.

Google Scholar: [Author Only](#) [Title Only](#) [Author and Title](#)

Wang, L., Cook, A., Patrick, J.W., Chen, X.Y., and Ruan, Y.L. (2014). Silencing the vacuolar invertase gene GhVIN1 blocks cotton fiber initiation from the ovule epidermis, probably by suppressing a cohort of regulatory genes via sugar signaling. *Plant J* 78, 686-696.

Google Scholar: [Author Only](#) [Title Only](#) [Author and Title](#)

Wang, Y.P., Zhang, N., Li, T., Yang, J.W., Zhu, X., Fang, C.X., Li, S.G., and Si, H.J. (2019). Genome-wide identification and expression analysis of StTCP transcription factors of potato (*Solanum tuberosum* L.). *Computational Biology and Chemistry* 78, 53-63.

Google Scholar: [Author Only](#) [Title Only](#) [Author and Title](#)

Weirauch, M.T., Yang, A., Albu, M., Cote, A.G., Montenegro-Montero, A., Drewe, P., Najafabadi, H.S., Lambert, S.A., Mann, I., Cook, K., Zheng, H., Goity, A., van Bakel, H., Lozano, J.C., Galli, M., Lewsey, M.G., Huang, E.Y., Mukherjee, T., Chen, X.T., Reece-Hoyes, J.S., Govindarajan, S., Shauly, G., Walhout, A.J.M., Bouget, F.Y., Ratsch, G., Larrondo, L.F., Ecker, J.R., and Hughes, T.R. (2014). Determination and inference of eukaryotic transcription factor sequence specificity. *Cell* 158, 1431-1443.

Google Scholar: [Author Only](#) [Title Only](#) [Author and Title](#)

Wu, L., Bhaskar, P.B., Busse, J.S., Zhang, R.F., Bethke, P.C., and Jiang, J.M. (2011). Developing cold-chipping potato varieties by silencing the vacuolar invertase gene. *Crop Sci.* 51, 981-990.

Google Scholar: [Author Only](#) [Title Only](#) [Author and Title](#)

Xie, K.B., Minkenberg, B., and Yang, Y.N. (2015). Boosting CRISPR/Cas9 multiplex editing capability with the endogenous tRNA-processing system. *Proc Natl Acad Sci USA* 112, 3570-3575.

Google Scholar: [Author Only](#) [Title Only](#) [Author and Title](#)

Xie, X.B., Li, S., Zhang, R.F., Zhao, J., Chen, Y.C., Zhao, Q., Yao, Y.X., You, C.X., Zhang, X.S., and Hao, Y.J. (2012). The bHLH transcription factor MdbHLH3 promotes anthocyanin accumulation and fruit colouration in response to low temperature in apples. *Plant Cell Environ* 35, 1884-1897.

Google Scholar: [Author Only](#) [Title Only](#) [Author and Title](#)

Ye, J., Shakya, R., Shrestha, P., and Rommens, C.M. (2010). Tuber-specific silencing of the acid invertase gene substantially lowers the acrylamide forming potential of potato. *J. Agric. Food Chem.* 58, 12162-12167.

Google Scholar: [Author Only](#) [Title Only](#) [Author and Title](#)

Yu, R.M., Chang, Y.N., Chen, H.Z., Feng, J.L., Wang, H.J., Tian, T., Song, Y.J., and Gao, G. (2022). Genome-wide identification of the GATA gene family in potato (*Solanum tuberosum* L.) and expression analysis. *Journal of Plant Biochemistry and Biotechnology* 31, 37-48.

Google Scholar: [Author Only](#) [Title Only](#) [Author and Title](#)

Yu, X.Y., Wang, X.F., Zhang, W.Q., Qian, T.T., Tang, G.M., Guo, Y.K., and Zheng, C.C. (2008). Antisense suppression of an acid invertase gene (*MAI1*) in muskmelon alters plant growth and fruit development. *J. Exp. Bot.* 59, 2969-2977.

Google Scholar: [Author Only](#) [Title Only](#) [Author and Title](#)

Zeng, Z.X., Zhang, W.L., Marand, A.P., Zhu, B., Buell, C.R., and Jiang, J.M. (2019). Cold stress induces enhanced chromatin accessibility and bivalent histone modifications H3K4me3 and H3K27me3 of active genes in potato. *Genome Biol* 20, 123.

Google Scholar: [Author Only](#) [Title Only](#) [Author and Title](#)

Zhang, C., Xie, C.-H., Song, B.-T., Liu, X., and Liu, J. (2008). RNAi effects on regulation of endogenous acid invertase activity in potato (*Solanum tuberosum* L.) tubers. *Chinese J. Agri. Biotech.* 5, 107-112.

Google Scholar: [Author Only](#) [Title Only](#) [Author and Title](#)

Zhang, H., Wu, T., Li, Z., Huang, K., Kim, N.E., Ma, Z.M., Kwon, S.W., Jiang, W.Z., and Du, X.L. (2021). OsGATA16, a GATA transcription factor, confers cold tolerance by repressing OsWRKY45-1 at the seedling stage in rice. *Rice* 14.

Google Scholar: [Author Only](#) [Title Only](#) [Author and Title](#)

Zhang, H., Liu, S.J., Ren, T.M., Niu, M.X., Liu, X., Liu, C., Wang, H.L., Yin, W.L., and Xia, X.L. (2023). Crucial abiotic stress regulatory network of NF-Y transcription factor in plants. *Int J Mol Sci* 24, 4426.

Google Scholar: [Author Only](#) [Title Only](#) [Author and Title](#)

Zhang, W.L., Zhang, T., Wu, Y.F., and Jiang, J.M. (2012). Genome-wide identification of regulatory DNA elements and protein-binding footprints using signatures of open chromatin in *Arabidopsis*. *Plant Cell* 24, 2719-2731.

Google Scholar: [Author Only](#) [Title Only](#) [Author and Title](#)

Zhao, H.N., Zhang, W.L., Chen, L.F., Wang, L., Marand, A.P., Wu, Y.F., and Jiang, J.M. (2018). Proliferation of regulatory DNA elements derived from transposable elements in the maize genome. *Plant Physiol* 176, 2789-2803.

Google Scholar: [Author Only](#) [Title Only](#) [Author and Title](#)

Zhao, H.N., Yang, M.Y., Bishop, J., Teng, Y.H., Cao, Y.X., Beall, B.D., Li, S.L., Liu, T.X., Fang, Q.X., Fang, C., Xin, H.Y., Nutzmans, H.W., Osbourn, A., Meng, F.L., and Jiang, J.M. (2022). Identification and functional validation of super-enhancers in *Arabidopsis thaliana*. *Proc Natl Acad Sci U S A* 119, e2215328119.

Google Scholar: [Author Only](#) [Title Only](#) [Author and Title](#)

Zhou, H., Zeng, R.F., Liu, T.J., Ai, X.Y., Ren, M.K., Zhou, J.J., Hu, C.G., and Zhang, J.Z. (2022). Drought and low temperature-induced NF-YA1 activates FT expression to promote citrus flowering. *Plant Cell Environ* 45, 3505-3522.

Google Scholar: [Author Only](#) [Title Only](#) [Author and Title](#)

Zhou, Q., Tang, D., Huang, W., Yang, Z.M., Zhang, Y., Hamilton, J.P., Visser, R.G.F., Bachem, C.W.B., Buell, C.R., Zhang, Z.H., Zhang, C.Z., and Huang, S.W. (2020). Haplotype-resolved genome analyses of a heterozygous diploid potato. *Nat Genet* 52, 1018-1023.

Google Scholar: [Author Only](#) [Title Only](#) [Author and Title](#)

Zhu, B., Zhang, W.L., Zhang, T., Liu, B., and Jiang, J.M. (2015). Genome-wide prediction and validation of intergenic enhancers in *Arabidopsis* using open chromatin signatures. *Plant Cell* 27, 2415-2426.

Google Scholar: [Author Only](#) [Title Only](#) [Author and Title](#)

Zhu, X.B., Richael, C., Chamberlain, P., Busse, J.S., Bussan, A.J., Jiang, J.M., and Bethke, P.C. (2014). Vacuolar invertase gene silencing in potato (*Solanum tuberosum* L.) improves processing quality by decreasing the frequency of sugar-end defects. *PLoS ONE* 9, e93381.

Google Scholar: [Author Only](#) [Title Only](#) [Author and Title](#)

Zhu, X.B., Gong, H.L., He, Q.Y., Zeng, Z.X., Busse, J.S., Jin, W.W., Bethke, P.C., and Jiang, J.M. (2016). Silencing of vacuolar invertase and asparagine synthetase genes and its impact on acrylamide formation of fried potato products. *Plant Biotechnol J* 14, 709-718.

Google Scholar: [Author Only](#) [Title Only](#) [Author and Title](#)

Zrenner, R., Schuler, K., and Sonnewald, U. (1996). Soluble acid invertase determines the hexose-to-sucrose ratio in cold-stored potato tubers. *Planta* 198, 246-252.

Google Scholar: [Author Only](#) [Title Only](#) [Author and Title](#)

ACCEPTED MANUSCRIPT